

Optical properties of diluted magnetic semiconductors and all-electrical control of individual dopant spins

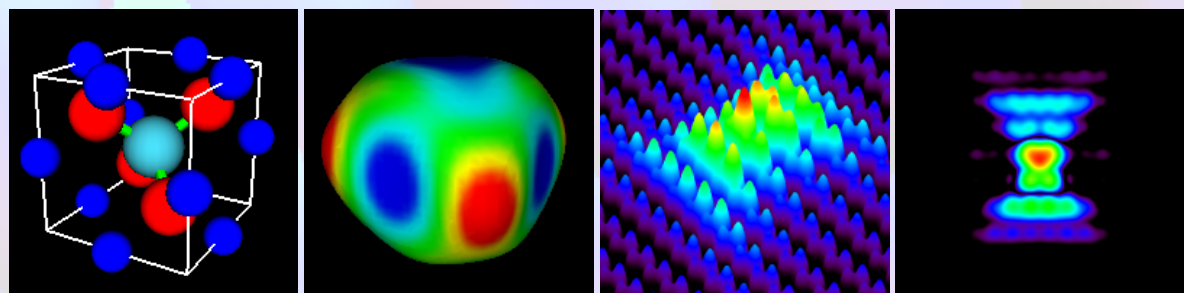
Jian-Ming Tang



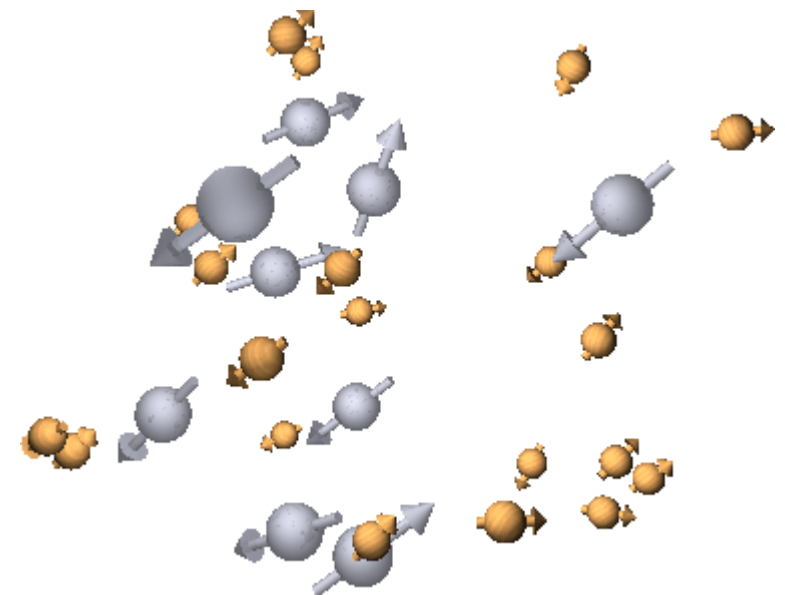
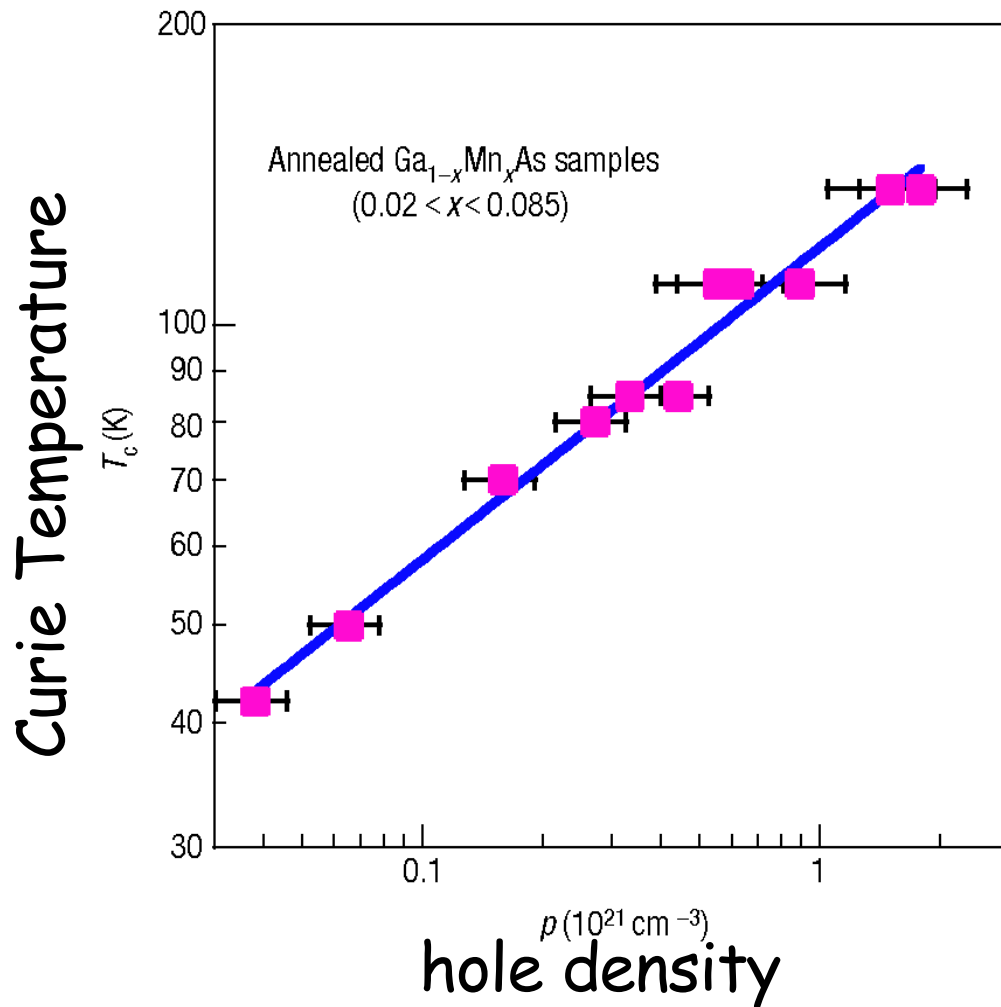
Department of Physics and Astronomy
Optical Science and Technology Center
University of Iowa



Supported by ARO



Carrier-mediated ferromagnetism



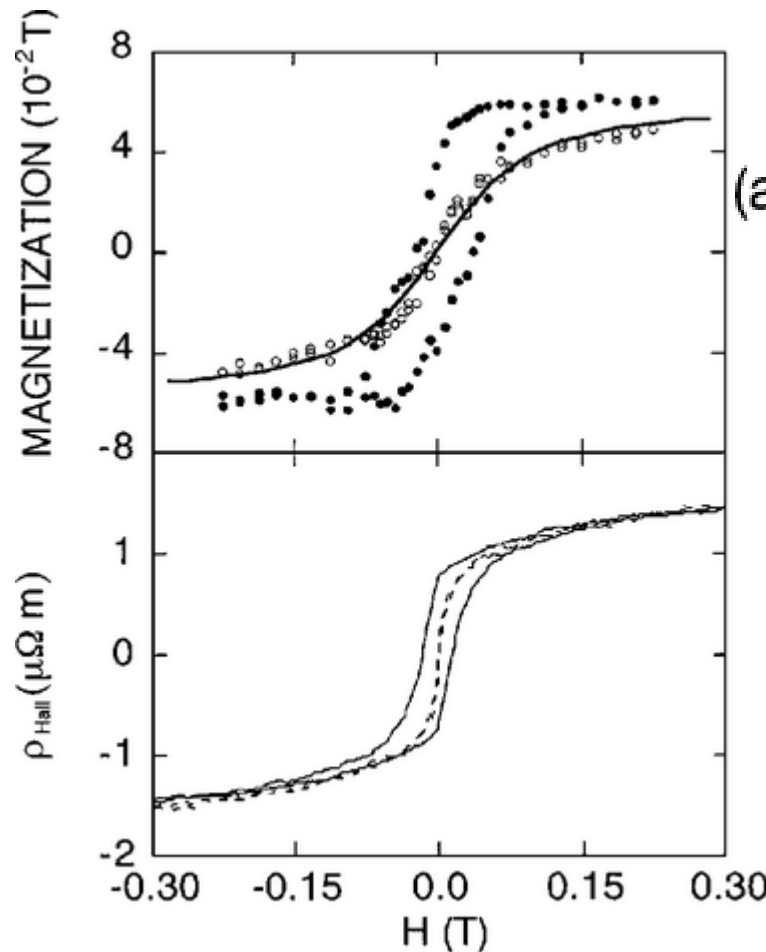
Mn:	$3d^5$	$4s^2$
Ga:		$4s^2$
As:		$4s^2$
		$4p^1$
		$4p^3$

K.C. Ku et al., APL 82, 2302 (2003)

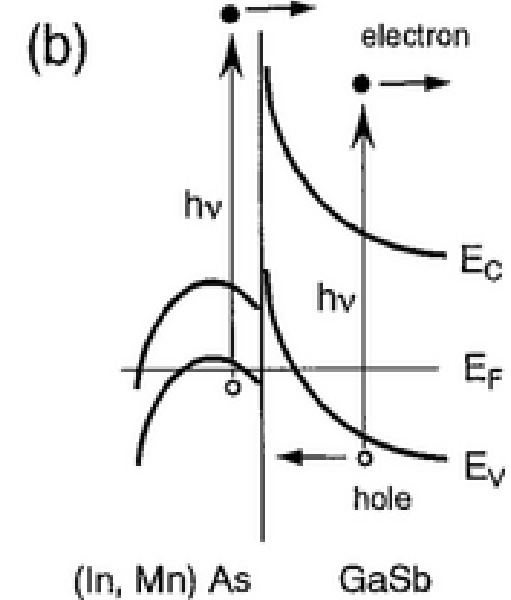
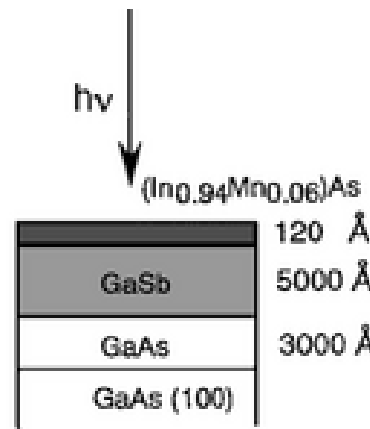
figure reprinted from A.H. MacDonald et al.

Nature Materials 4, 195 (2005)

Light-induced ferromagnetic order

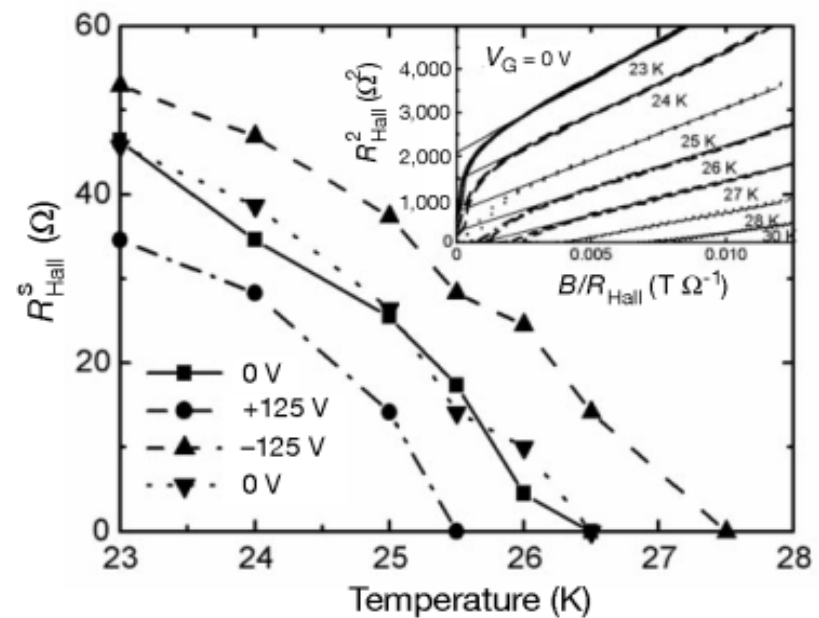
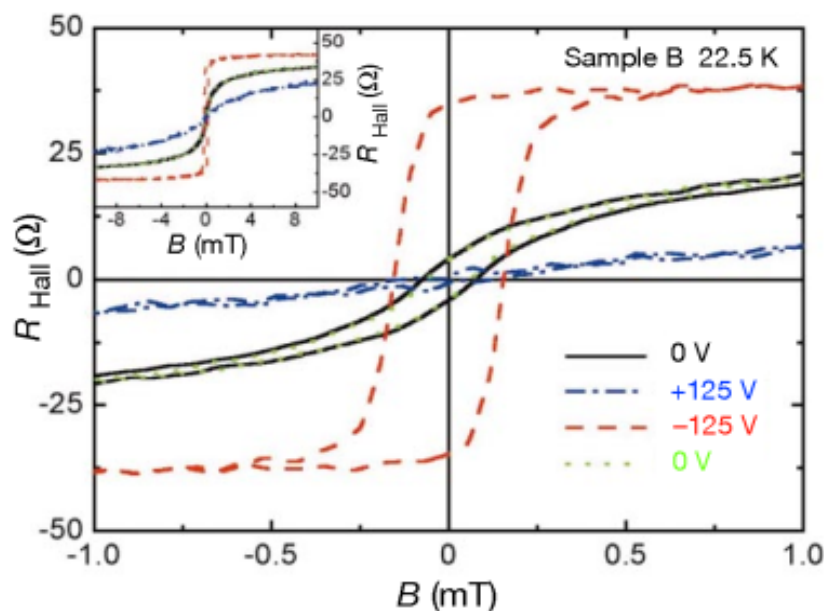
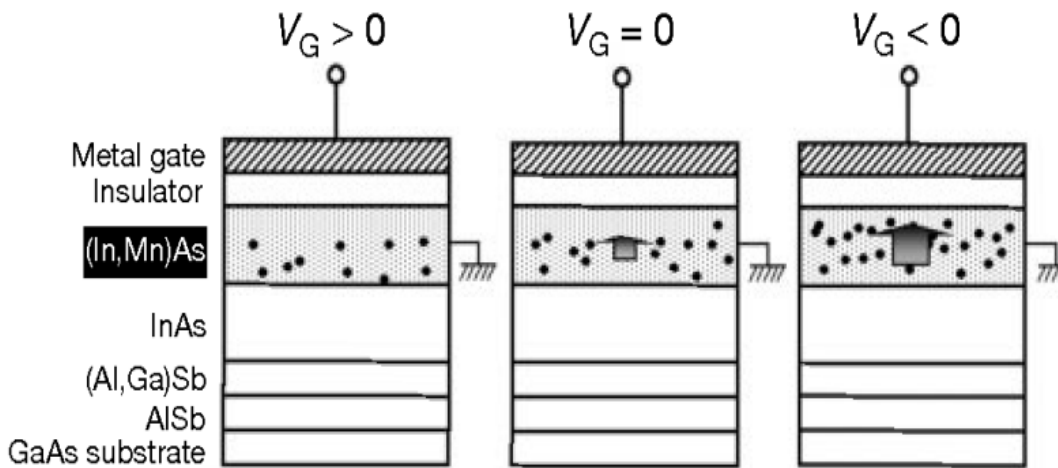


$T = 5\text{ K}$



S. Koshihara et al., PRL 78, 4617 (1997)

Electric-field control of ferromagnetism



Outline

- Theory of single magnetic dopants
- magnetic circular dichroism in optical absorption
- electrical manipulation of single Mn spins

Collaborators

- Theory

- Michael E. Flatté

- University of Iowa, USA

- Jeremy Levy

- University of Pittsburgh, USA

- Experiment

- Andrei M. Yakunin, Andrei Yu. Silov, Paul M. Koenraad, Joachim H. Wolter

- Eindhoven University of Technology, The Netherlands

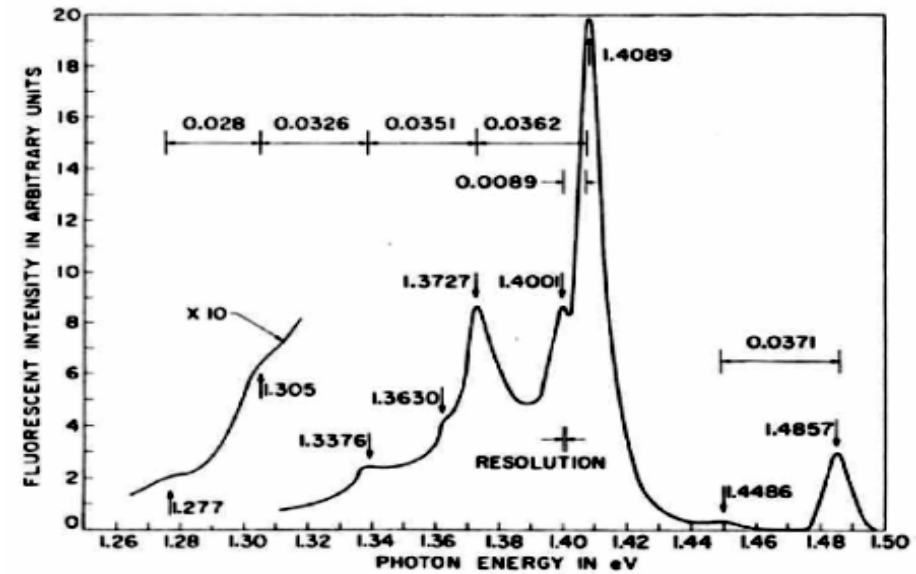
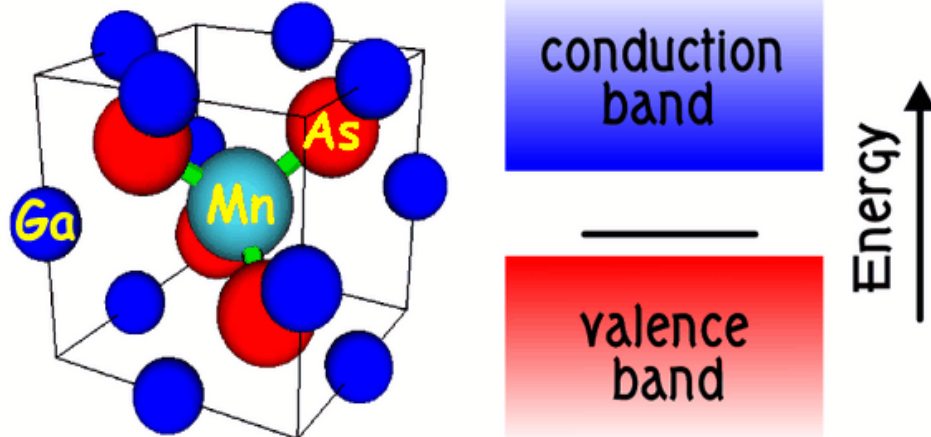
- Wim Van Roy, Joe De Boeck

- Interuniversity Micro-Electronics Center, Belgium

- Dale S. Kitchen, Anthony Richardella, Ali Yazdani

- Princeton University

Mn_{Ga} is an acceptor in GaAs

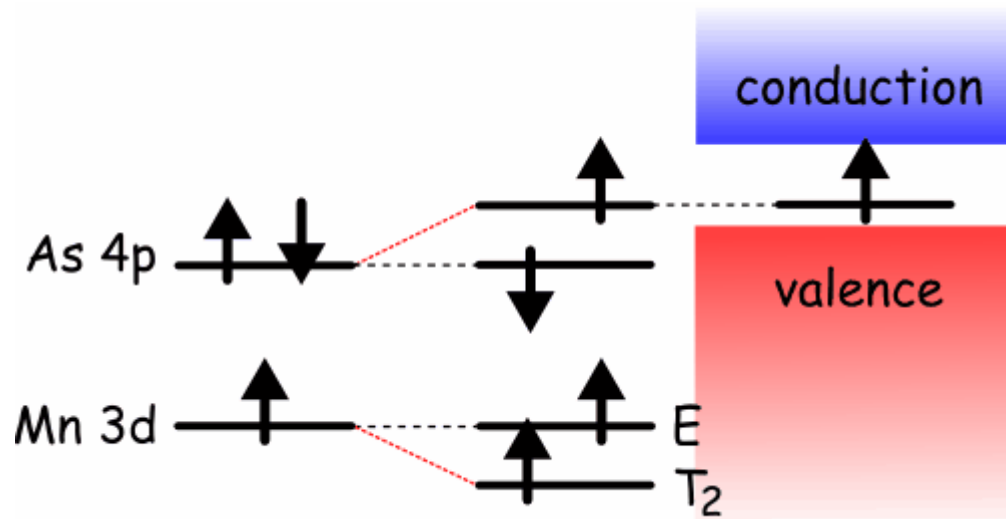


T.C. Lee and W.W. Anderson,
Solid State Commun. 2, 265 (1964)

	Cr	Mn	Fe	Co
GaP (2.3)	1	0.4	0.8	0.4
GaAs (1.5)	0.6	0.1	0.5	0.1
InP (1.4)	1	0.2	0.8	0.3
InAs (0.4)		0.03		

(unit: eV)

Antiferromagnetic p-d hybridization



P. Vogl and J.M. Baranowski,
Acta. Phys. Polon. A67, 133 (1985)

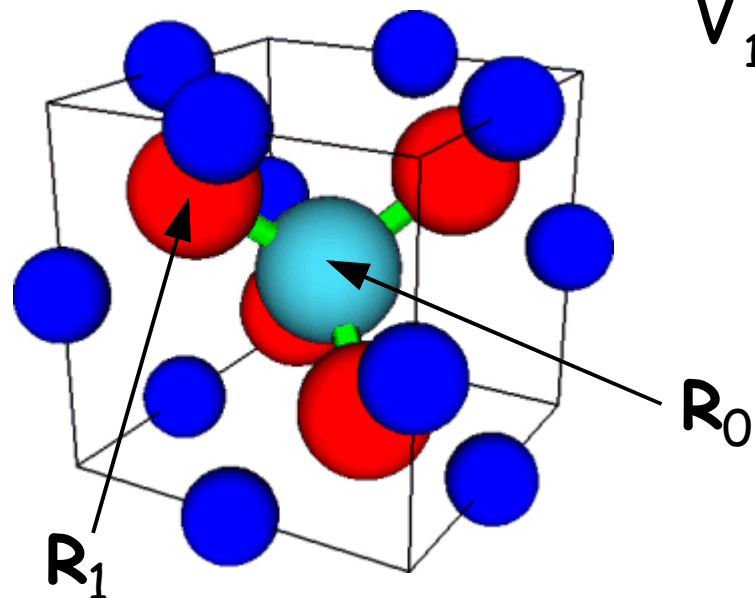
- "Hydrogenic" levels
 - 25.6 meV in GaAs
 - 16.6 meV in InAs
- A. Baldereschi and N.O. Lipari
Phys. Rev. 8, 2697 (1973)
- Mn level:
 - 113 meV in GaAs
 - 28 meV in InAs

Semiclassical exchange model

$$V(\mathbf{R}, \mathbf{R}') = \left[V_0 \sum_{\ell\sigma} c_{\ell\sigma}^\dagger(\mathbf{R}_0) c_{\ell\sigma}(\mathbf{R}_0) + V_1 \sum_{\ell j} c_{\ell\uparrow}^\dagger(\mathbf{R}_j) c_{\ell\uparrow}(\mathbf{R}_j) \right] \delta_{\mathbf{R}, \mathbf{R}'}$$

$$V_0 = 1 \text{ eV}$$

$$V_1 = 3.59 \text{ eV}$$



- Coulomb potential ($\sim 1/\epsilon r$)
 - 0.5 eV at \mathbf{R}_1
- effective mass model
 - acceptor level: 25.6 meV
- Mn level: 113 meV

$$|\psi(\mathbf{R}_0)|^2 \sim 0.1$$

$$|\psi(\mathbf{R}_1)|^2 \sim 0.05$$

Koster-Slater approach

$$H = H_0 + V_{\text{impurity}}$$

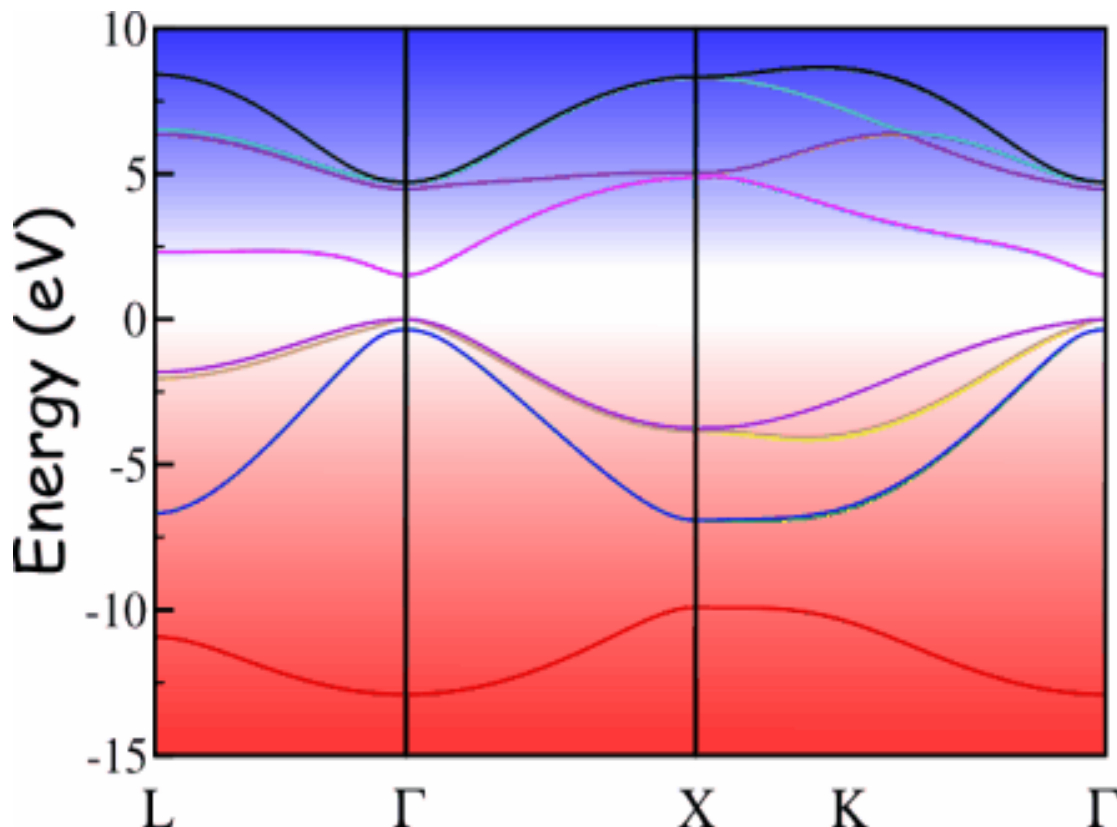
$$\hat{G}_0(\mathbf{k}; \omega) = [\omega - \hat{H}_0(\mathbf{k}) \pm i\varepsilon]^{-1}$$

$$\hat{G}_0(\mathbf{R}, \mathbf{R}'; \omega) = \Omega_{\mathbf{k}}^{-1} \int d^3k \hat{G}_0(\mathbf{k}; \omega) e^{i\mathbf{k}\cdot(\mathbf{R}-\mathbf{R}')}$$

$$\begin{aligned} \hat{G}(\mathbf{R}, \mathbf{R}'; \omega) &= \hat{G}_0(\mathbf{R}, \mathbf{R}'; \omega) \\ &\quad + \sum_{\mathbf{R}_a, \mathbf{R}_b} \hat{G}(\mathbf{R}, \mathbf{R}_a; \omega) \hat{V}(\mathbf{R}_a, \mathbf{R}_b) \hat{G}_0(\mathbf{R}_b, \mathbf{R}'; \omega) \\ \hat{G}(\omega) &= [\hat{1} - \hat{G}_0(\omega) \hat{V}]^{-1} \hat{G}_0 \end{aligned}$$

- G.F. Koster and J.C. Slater, PR 95, 1167 (1954)
- H.P. Hjalmarson, P. Vogl, D.J. Wolford and J.D. Dow, PRL 44, 810 (1980)
- J.-M. Tang and M.E. Flatté, PRL 92, 047201 (2004)

$H_0(k)$ (sp^3 tight-binding model)

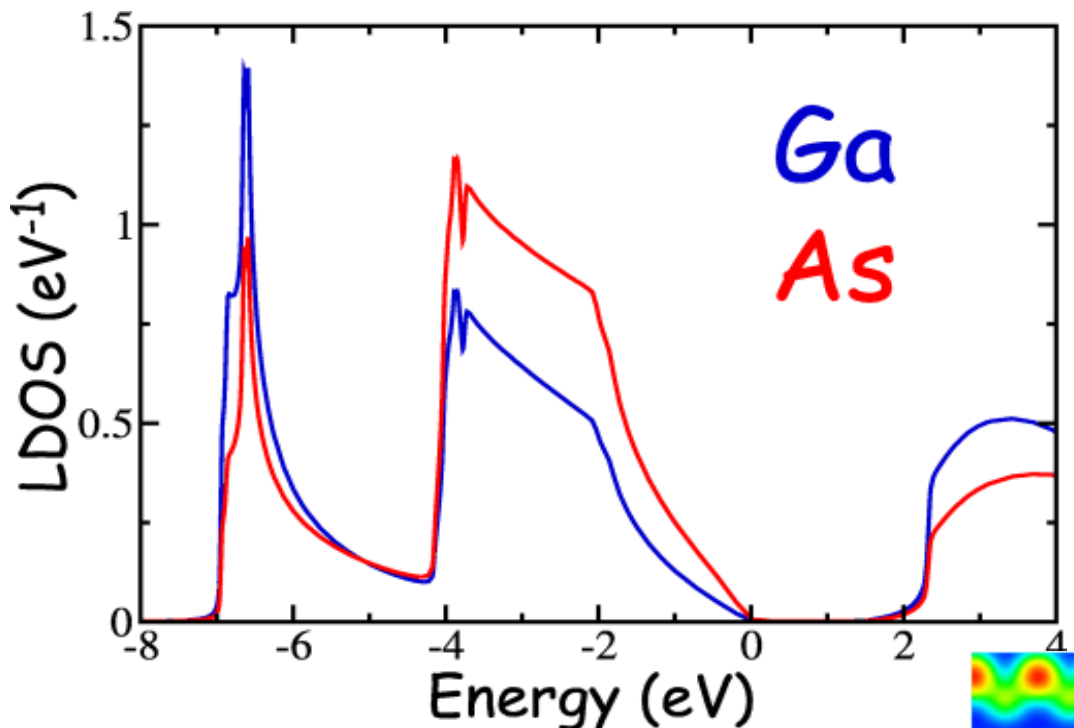


- full-zone band structure
 - spatial structure at atomic scales
 - crystal symmetry
- spin-orbit interaction

D. J. Chadi, PRB 16, 790 (1977)

- Atomic orbital basis: $\phi_{\ell,s}(\mathbf{R})$
 - minimum set for zincblende lattice: 16 basis states
2 (atomic sites) \times 4 (sp^3 orbitals) \times 2 (spins)
- nearest-neighbor interaction
- on-site spin-orbit interaction

Local density of states (LDOS)



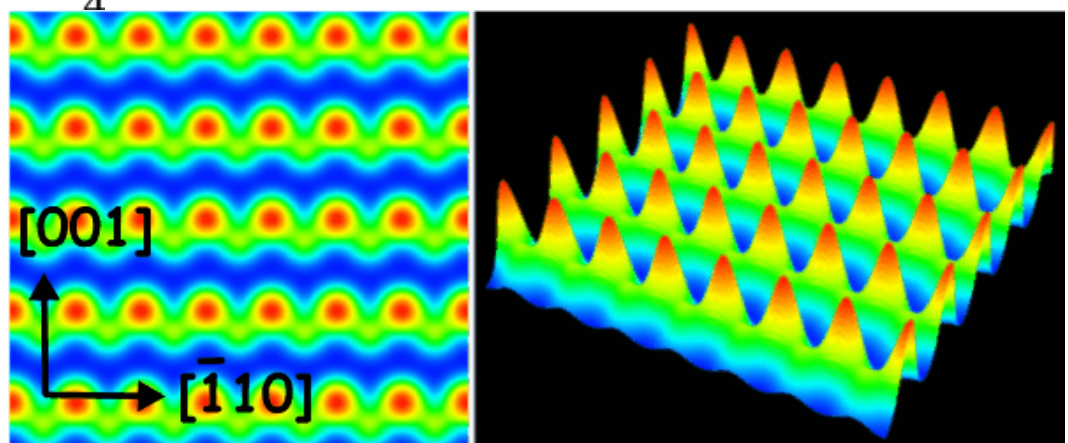
- density of states

$$D(E) = \sum_n \delta(E - E_n)$$

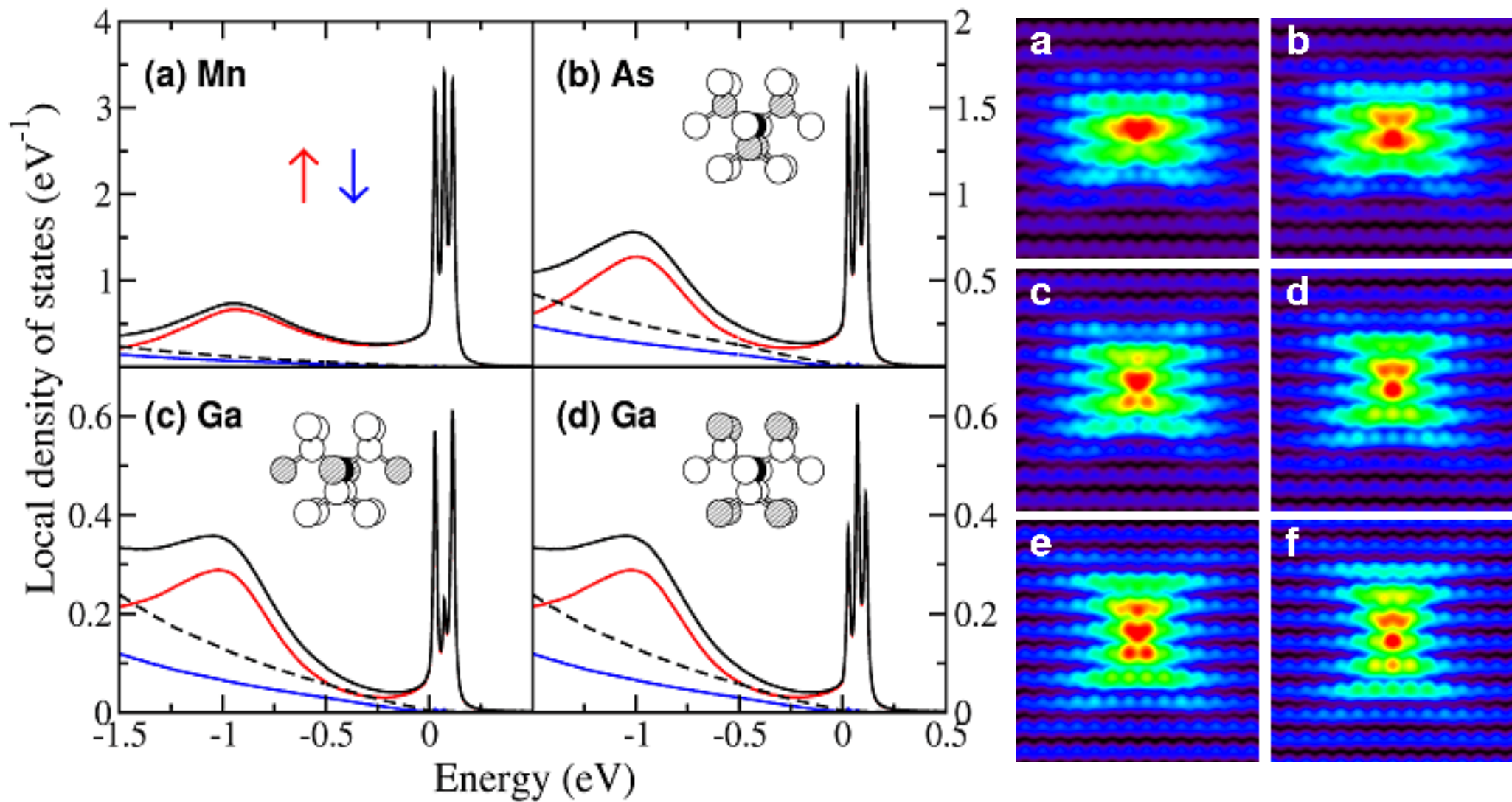
$LDOS(r, E)$

$$= \sum_n |\Psi_n(r)|^2 \delta(E - E_n)$$

$$\approx -\frac{1}{\pi} \Im \left[\sum_{\mathbf{R}, \alpha} \hat{G}_{\alpha, \alpha}(\mathbf{R}, \mathbf{R}; E) |\phi_\alpha(\mathbf{r} - \mathbf{R})|^2 \right]$$

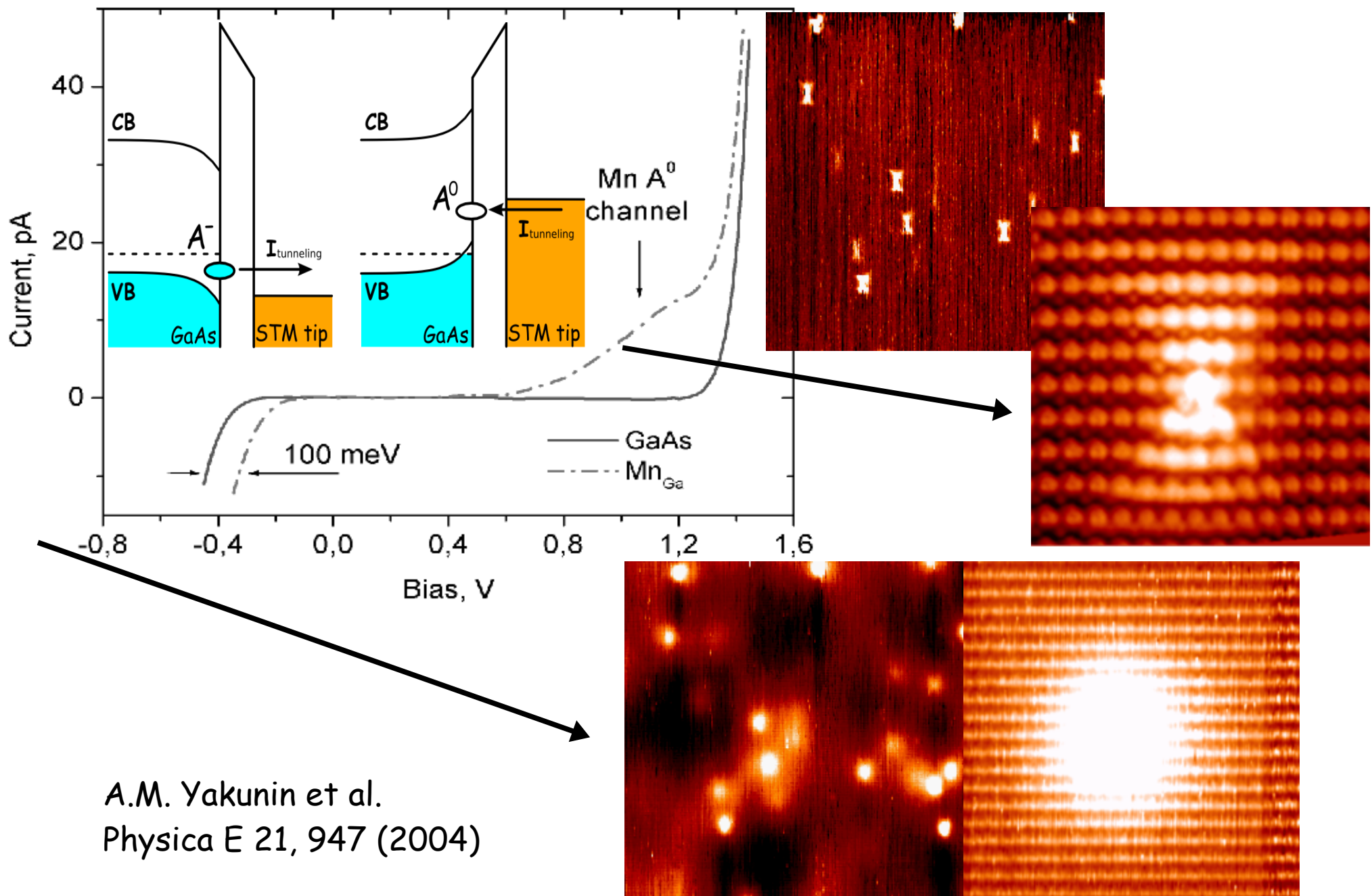


LDOS near a Mn dopant

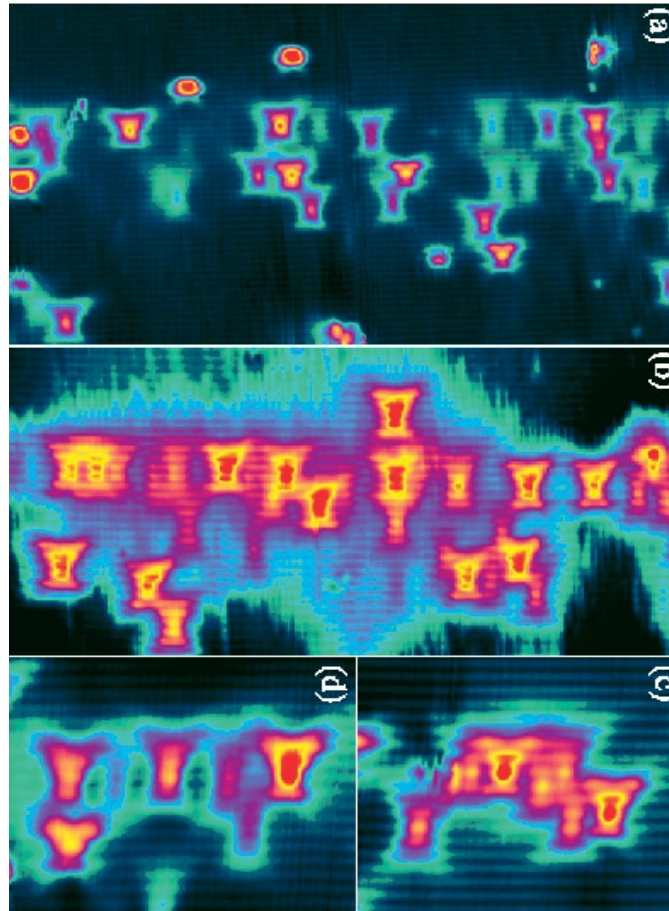
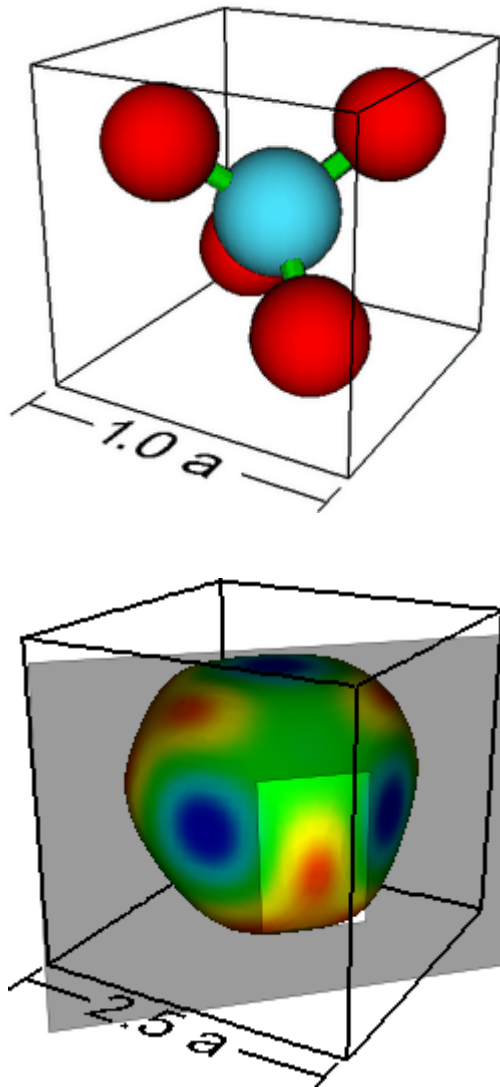


J.-M. Tang and M. E. Flatté, PRL 92, 047201 (2004)

Scanning Tunneling Microscopy



Mn acceptor wavefunction



A.M. Yakunin et al.,
PRL 95, 256402 (2005)

Magnetic circular dichroism in optical absorption

Optical absorption in bulk semiconductors

- Momentum is a good quantum number
- Interband transitions

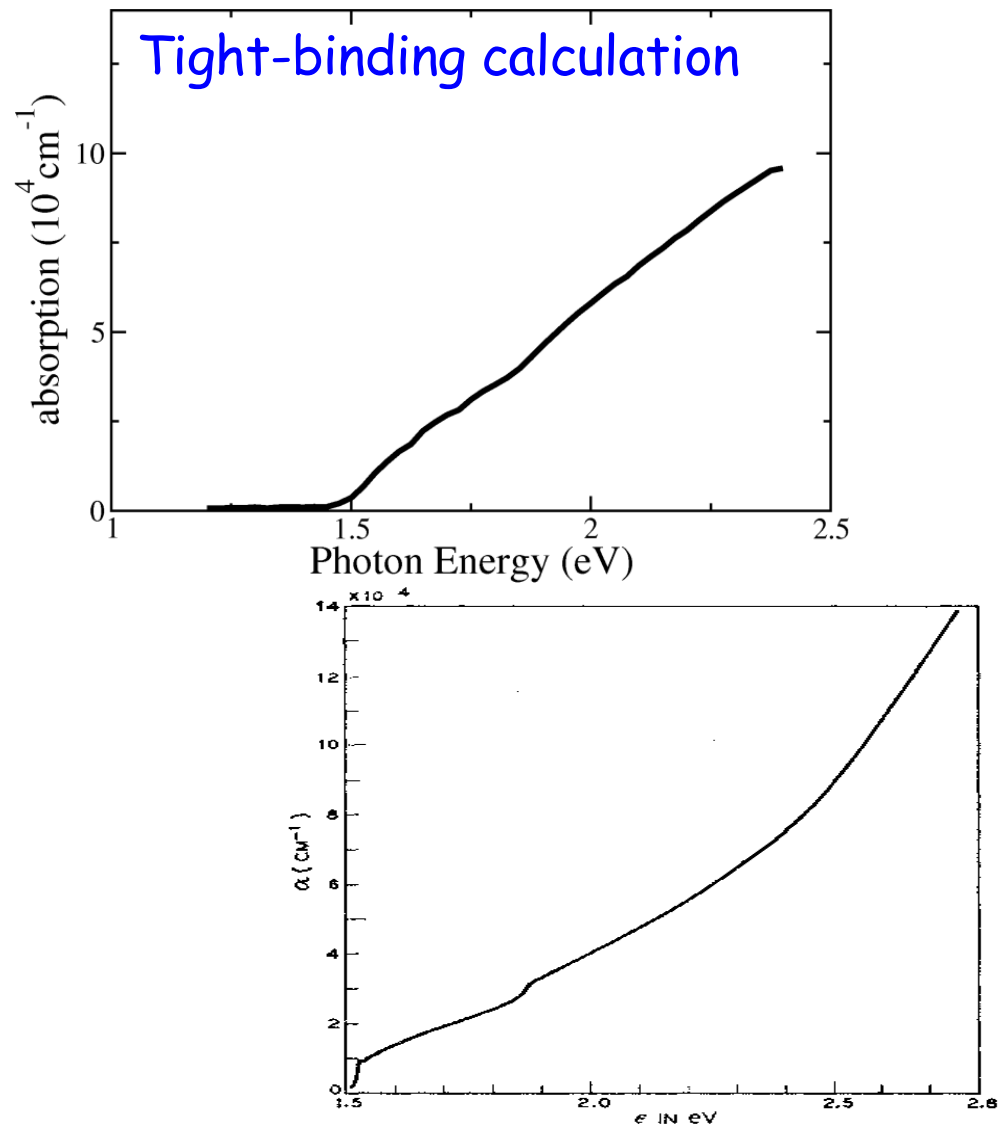
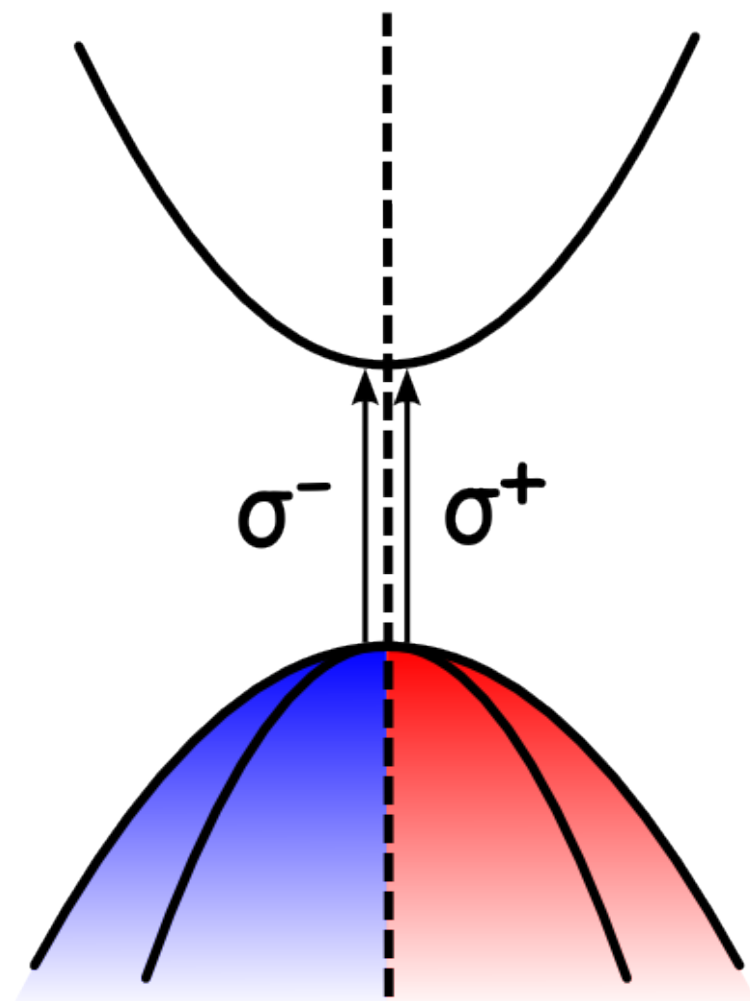
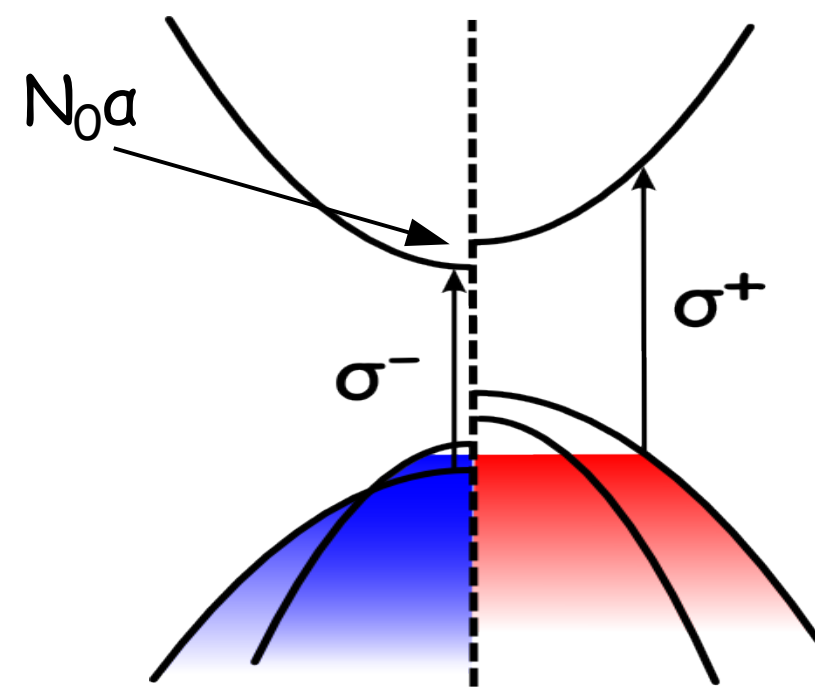
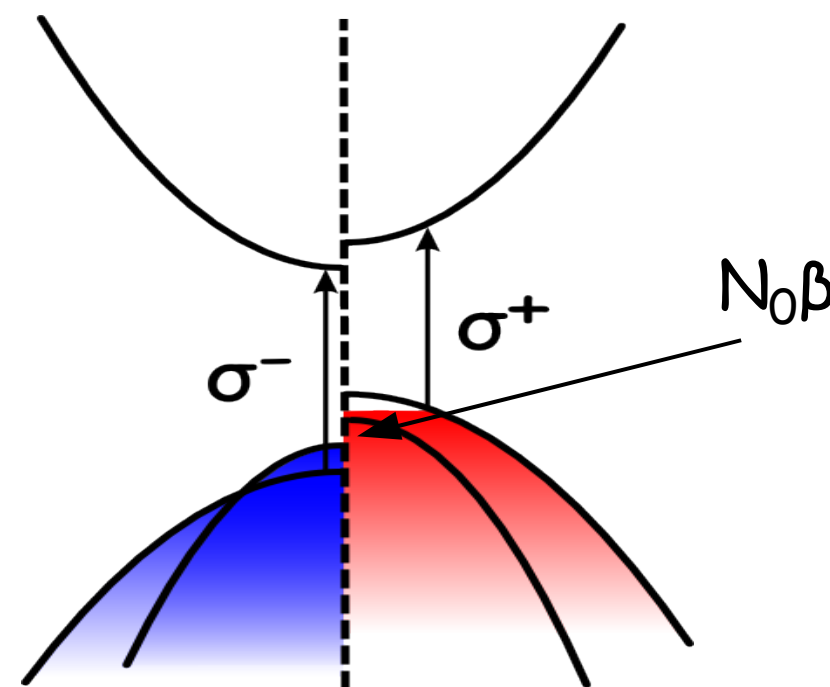
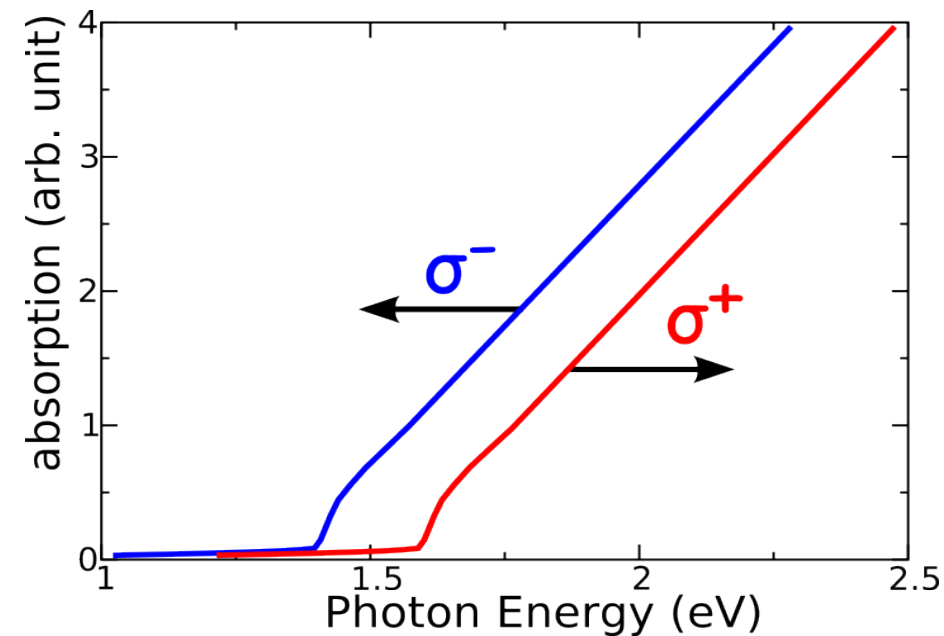
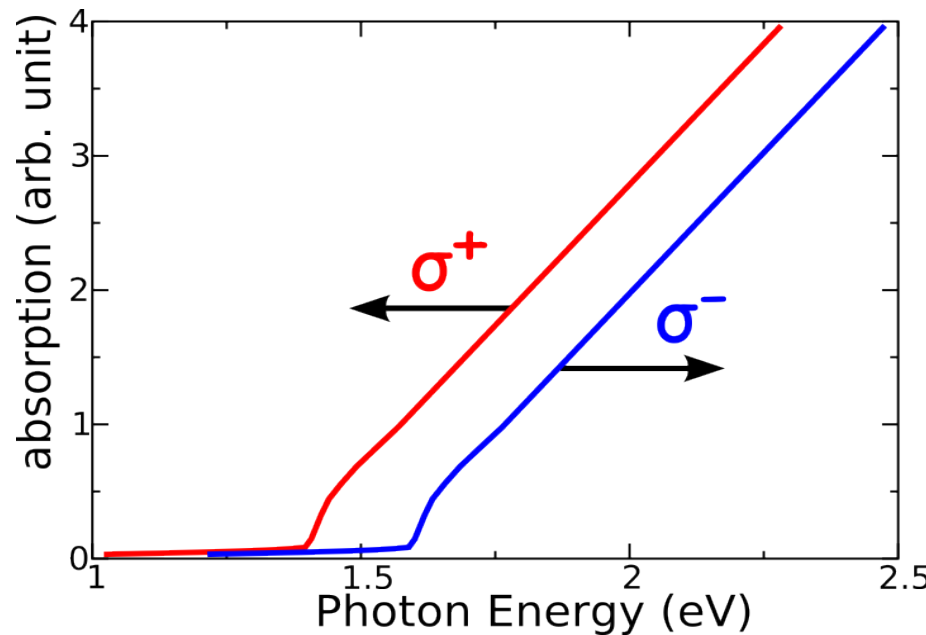
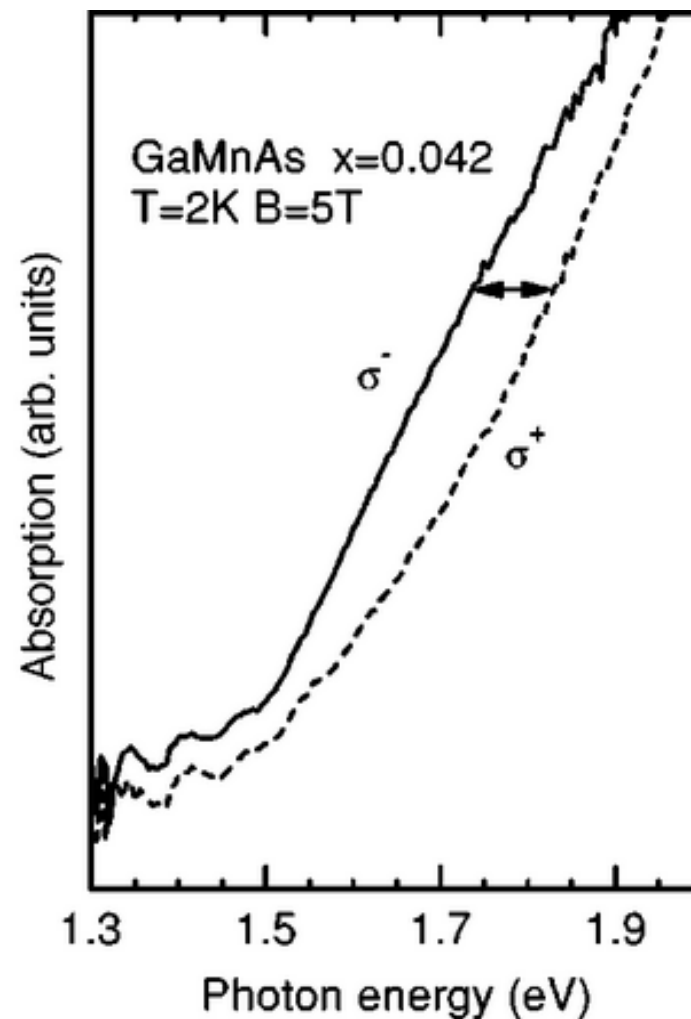
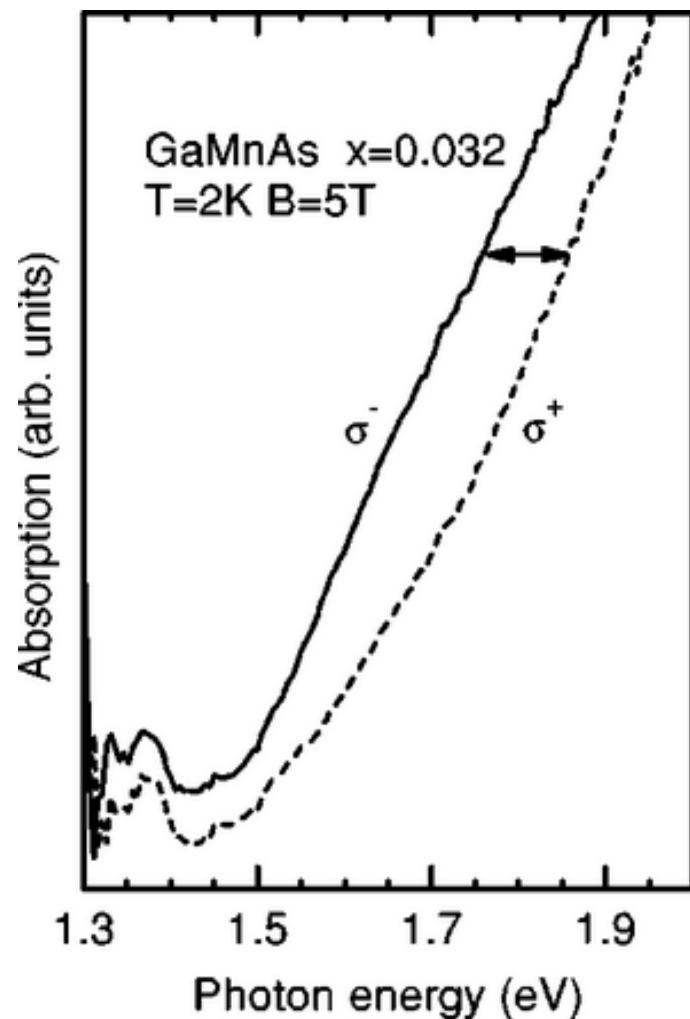


FIG. 6. Absorption of GaAs at 21°K.
M.D. Sturge, Phys. Rev. 137, 768 (1962)

Exchange splitting and Moss-Burnstein shift

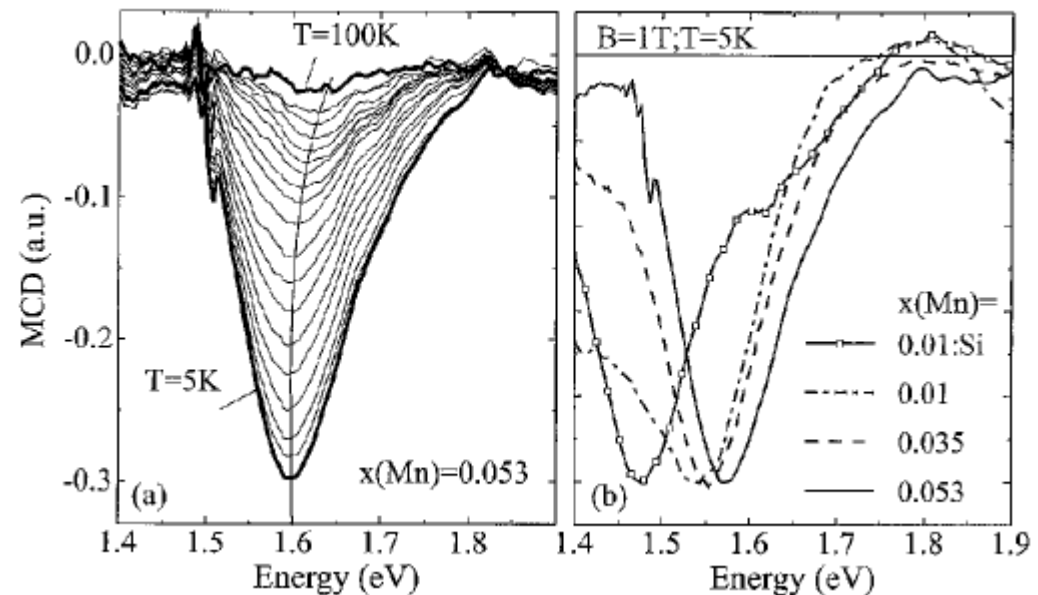
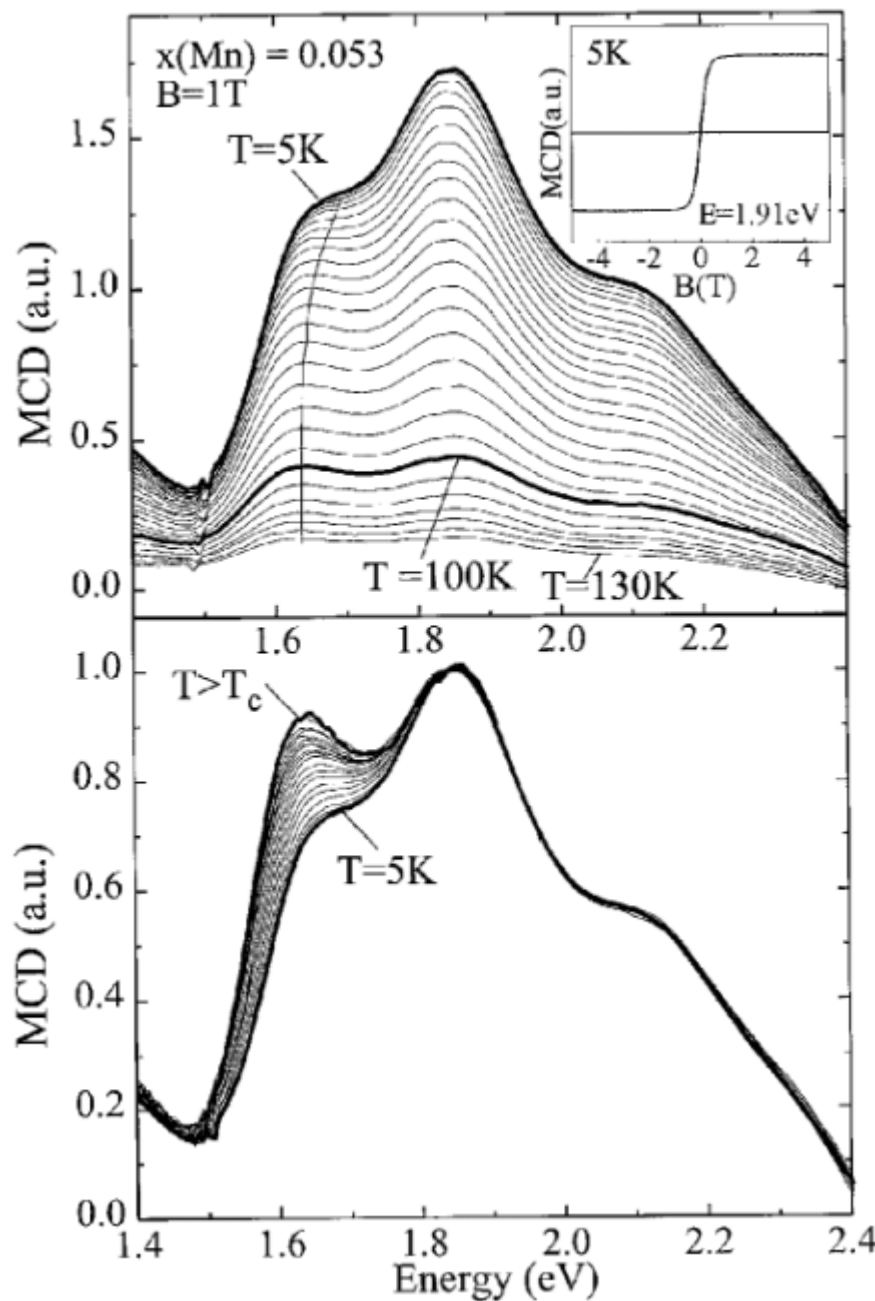


Magneto-optical absorption



J. Szczytko et al., PRB 59, 12935 (1999)

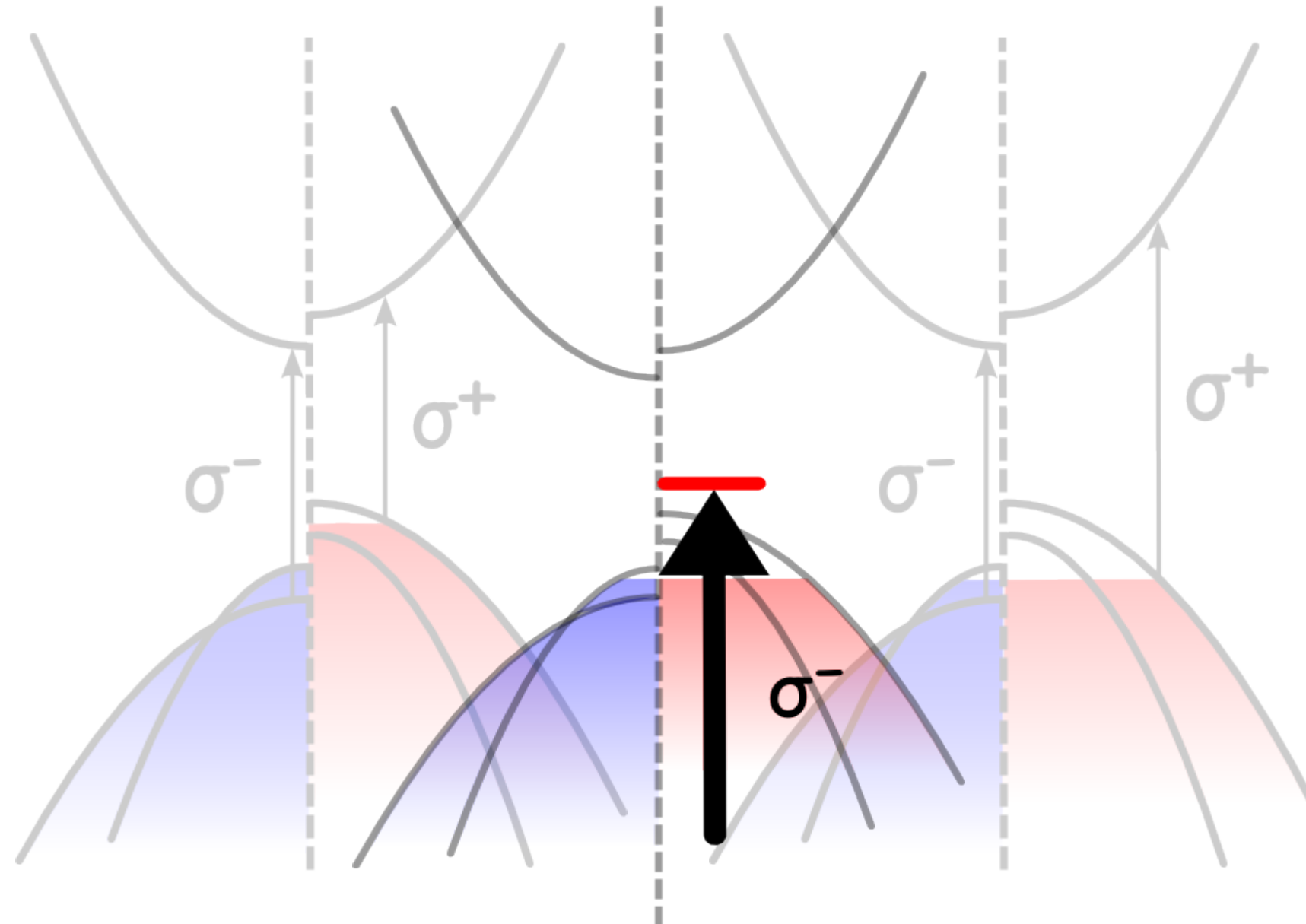
Magnetic circular dichroism

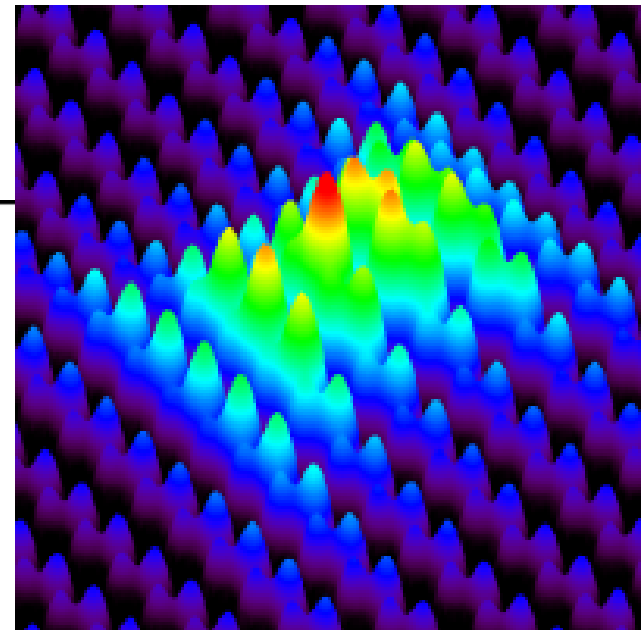
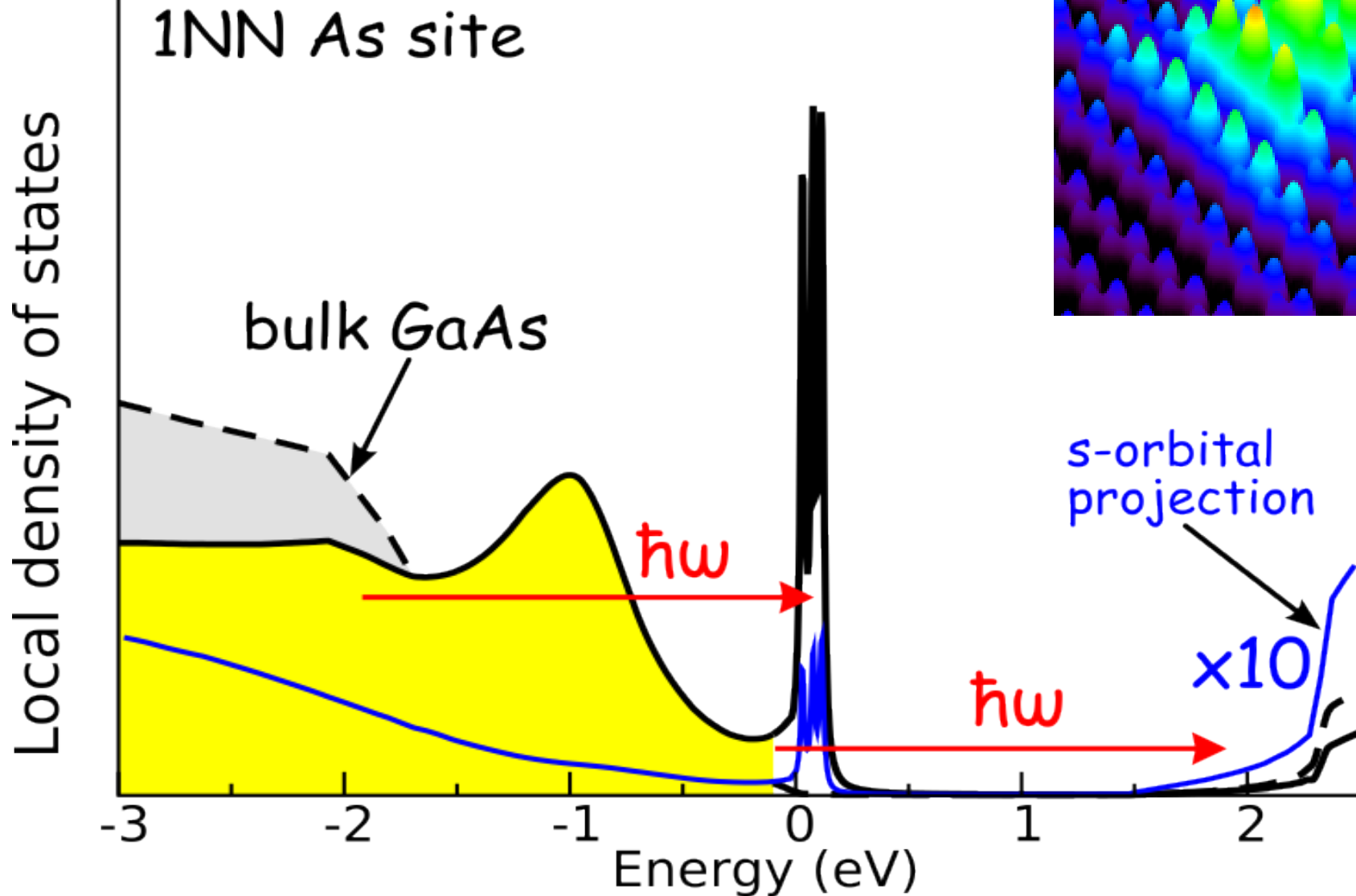


$$MCD = \frac{\alpha^- - \alpha^+}{\alpha^- + \alpha^+}$$

B. Beschoten et al., PRL 83, 3073 (1999)

Momentum is not a good quantum number





absorption coefficients

$$\hat{G}_0^A(\mathbf{k}; \omega) = [\omega - \hat{H}_0(\mathbf{k}) \pm \varepsilon]^{-1}$$

$$\hat{G}^R(\mathbf{R}, \mathbf{R}'; \omega) = \hat{G}_0(\mathbf{R}, \mathbf{R}'; \omega) + \sum_{\mathbf{R}_a, \mathbf{R}_b} \hat{G}(\mathbf{R}, \mathbf{R}_a; \omega) \hat{V}(\mathbf{R}_a, \mathbf{R}_b) \hat{G}_0(\mathbf{R}_b, \mathbf{R}'; \omega)$$

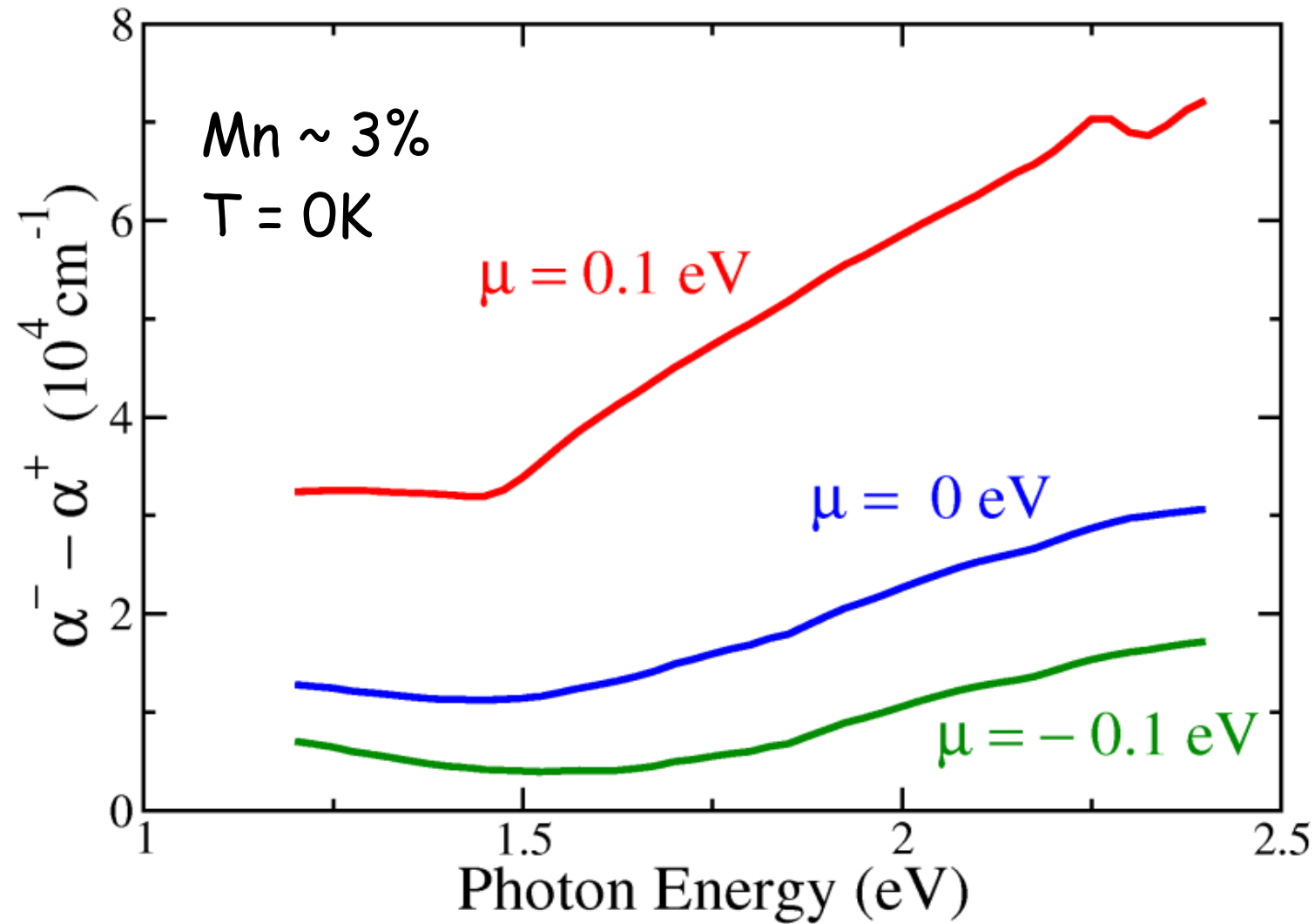
$$\alpha^\pm = \frac{\pi e^2}{(2\pi)^2 V n \varepsilon_0 m^2 \omega_C} \int dE_f \int dE_i f(E_i) [1 - f(E_f)] \delta(E_f - E_i - \hbar\omega)$$

$$\times \text{Tr} \sum_{\mathbf{R}_1, \mathbf{R}_2, \mathbf{R}_3, \mathbf{R}_4} [\hat{G}^R(\mathbf{R}_1, \mathbf{R}_2; E_i) - \hat{G}^A(\mathbf{R}_1, \mathbf{R}_2; E_i)] \langle \phi(\mathbf{R}_2) | \hat{P}^{\pm\dagger} | \phi(\mathbf{R}_3) \rangle$$

$$\times [\hat{G}^A(\mathbf{R}_3, \mathbf{R}_4; E_f) - \hat{G}^R(\mathbf{R}_3, \mathbf{R}_4; E_f)] \langle \phi(\mathbf{R}_4) | \hat{P}^{\pm} | \phi(\mathbf{R}_1) \rangle$$

approximation: only on-site momentum matrix element

Magnetic circular dichroism



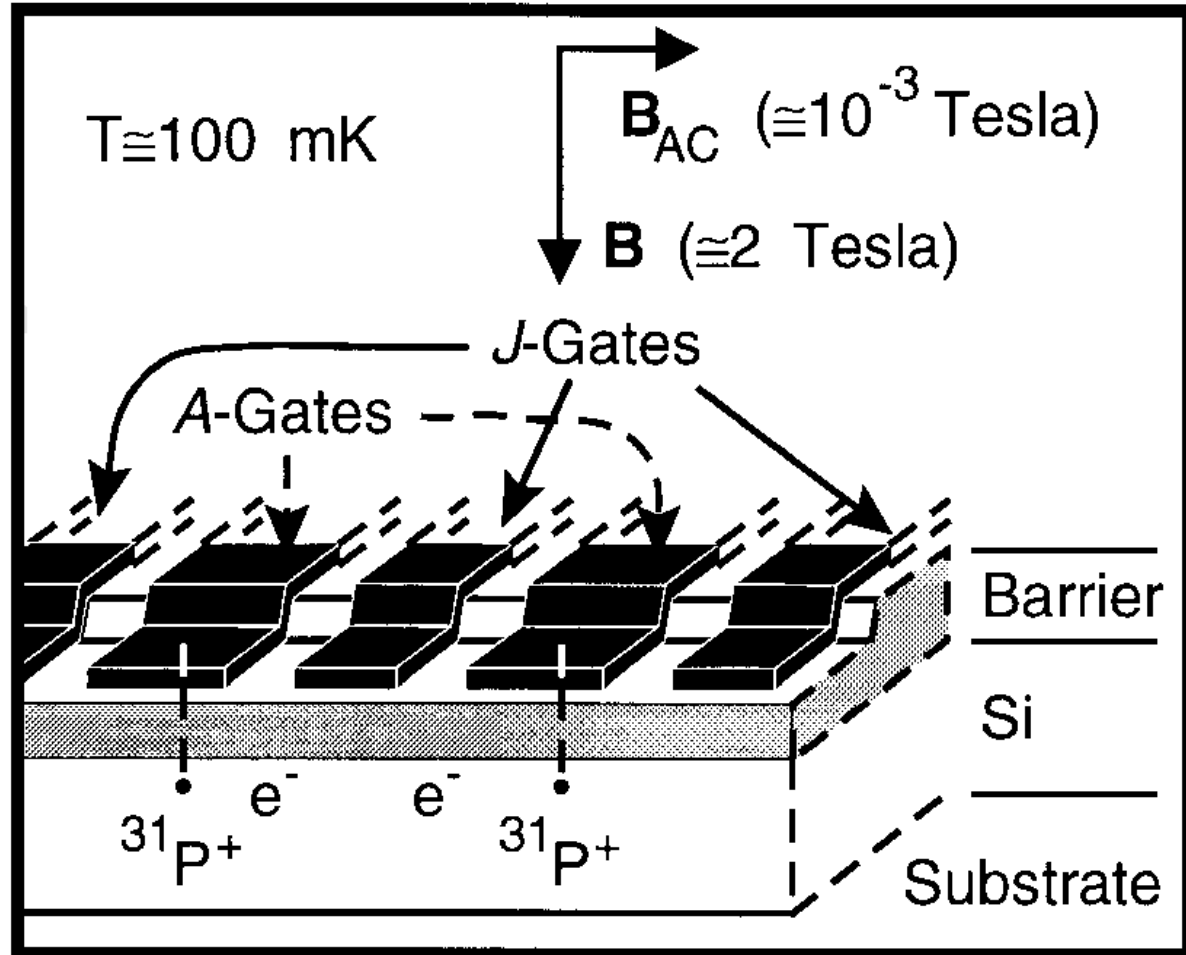
Summary

- A new theoretical tool for calculating optical processes in the presence of impurity band
- Optical transitions from the valence band to the impurity band are the main contribution to the magnetic circular dichroism in diluted magnetic semiconductors

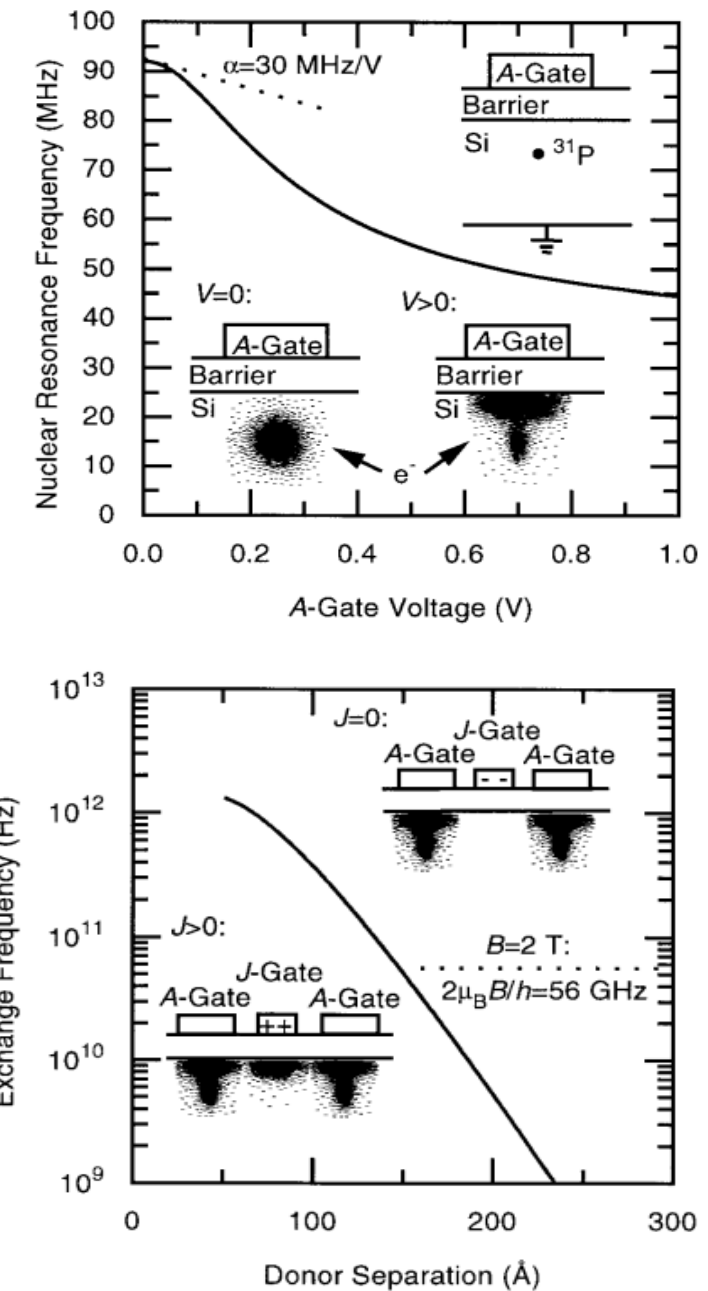
Electrical manipulation of single Mn spins

J.-M. Tang, J. Levy, and M. E. Flatté
quant-ph/0605203

Si:P quantum computer



B. E. Kane, Nature 393, 133 (1998)



Electrical manipulation of electron spins

- Gigahertz electron spin manipulation using voltage-controlled g-tensor modulation
Y. Kato et al., Science 299, 1201 (2003)
- Coherent manipulation of coupled electron spins in semiconductor quantum dots
J. R. Petta et al., Science 309, 2180 (2005)

Quantum computation

- qubit
- initialization
 - apply a dc magnetic field to split spin states
- control
 - apply an ac magnetic field to flip spin
 - two-qubit operation
- detection

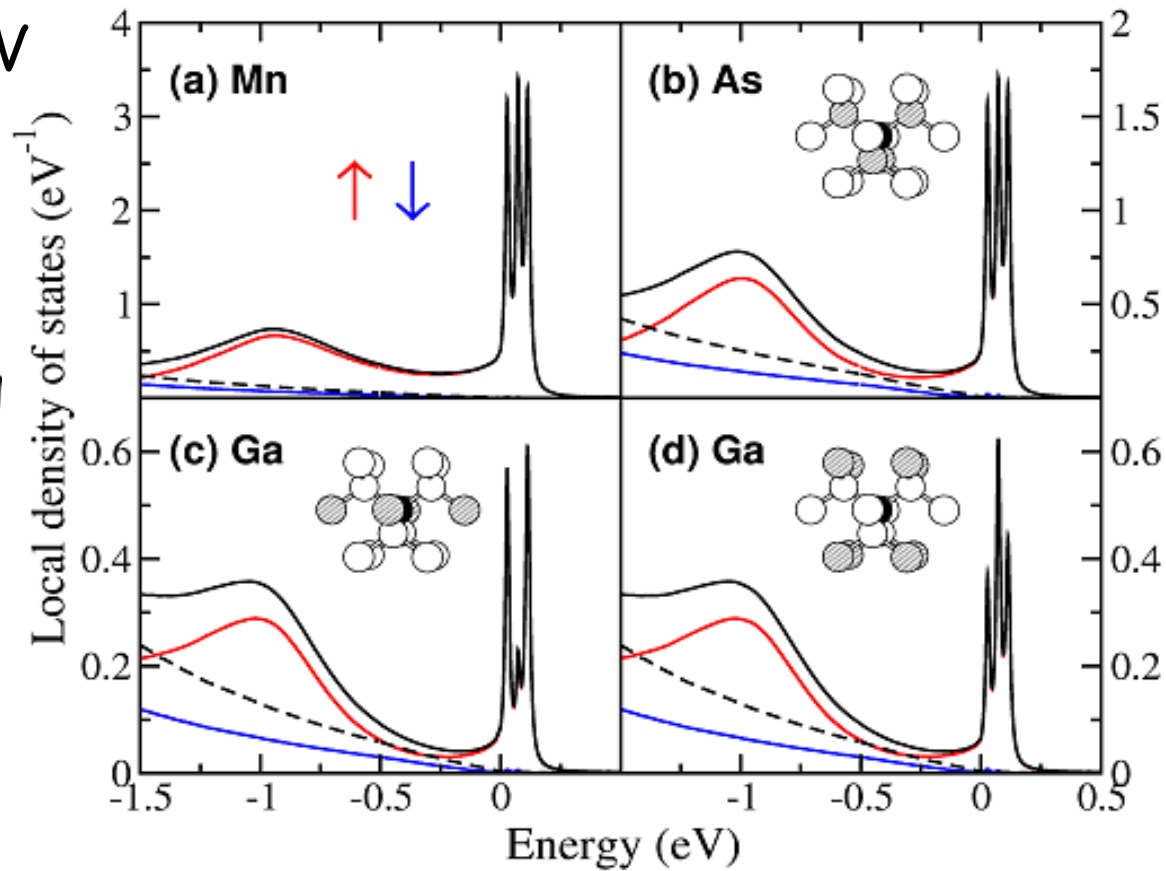
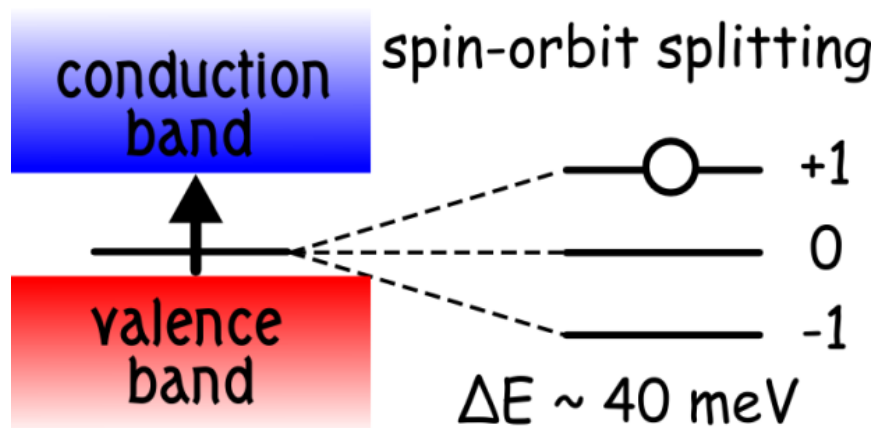
Quantum spin states

$$H_{\text{eff}} = A \mathbf{S}_{\text{Mn}} \cdot \mathbf{s}_h + B \mathbf{s}_h \cdot \ell_h$$

$$S_{\text{Mn}} = 5/2, \ell_h = 1, s_h = \frac{1}{2}$$

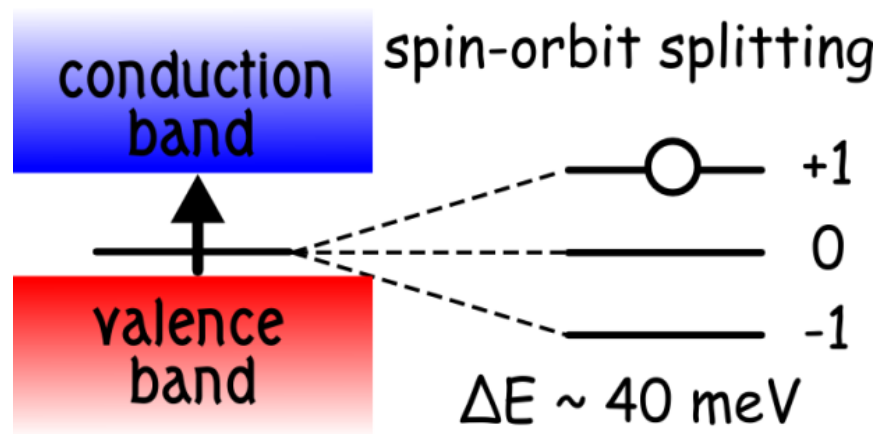
$$A \sim -300 \text{ meV}, B \sim 80 \text{ meV}$$

$$A < 0, B > 0, |A| \gg |B|$$

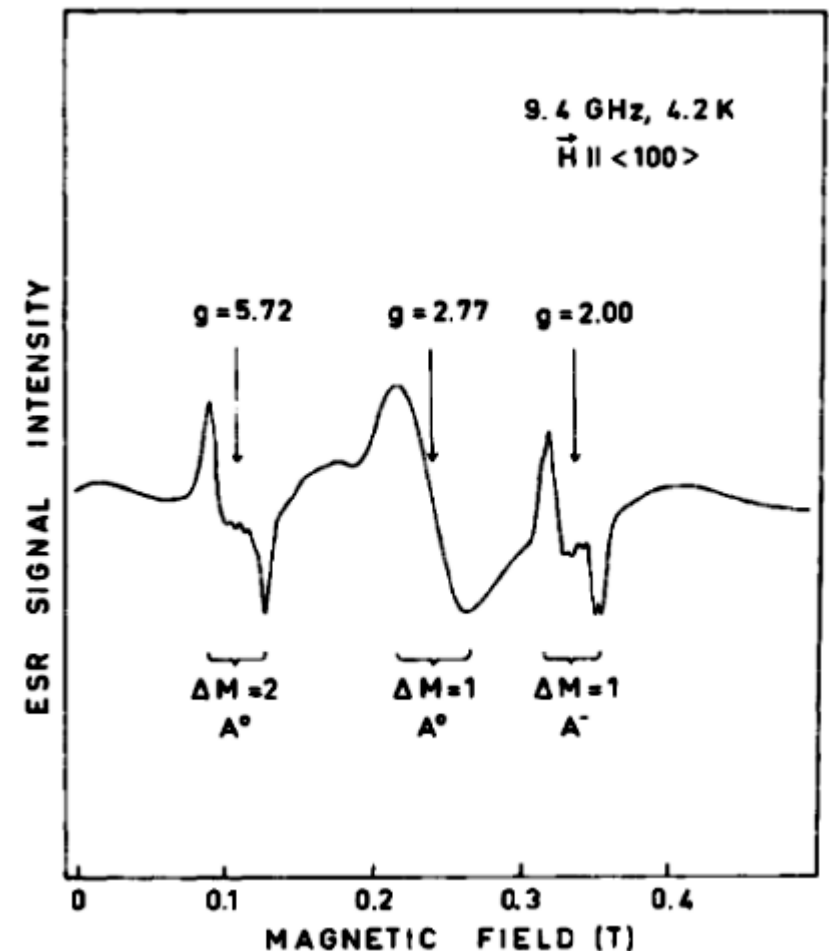
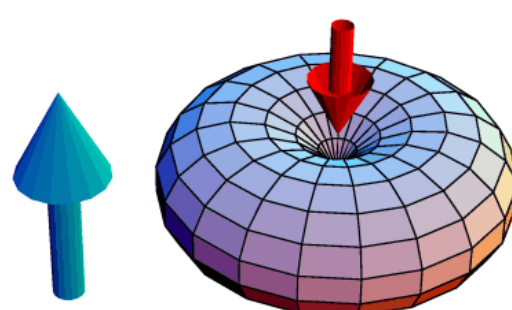


(Mn+hole) is a J=1 complex

$$H_{\text{eff}} = A \mathbf{S}_{\text{Mn}} \cdot \mathbf{s}_h + B \mathbf{s}_h \cdot \ell_h$$



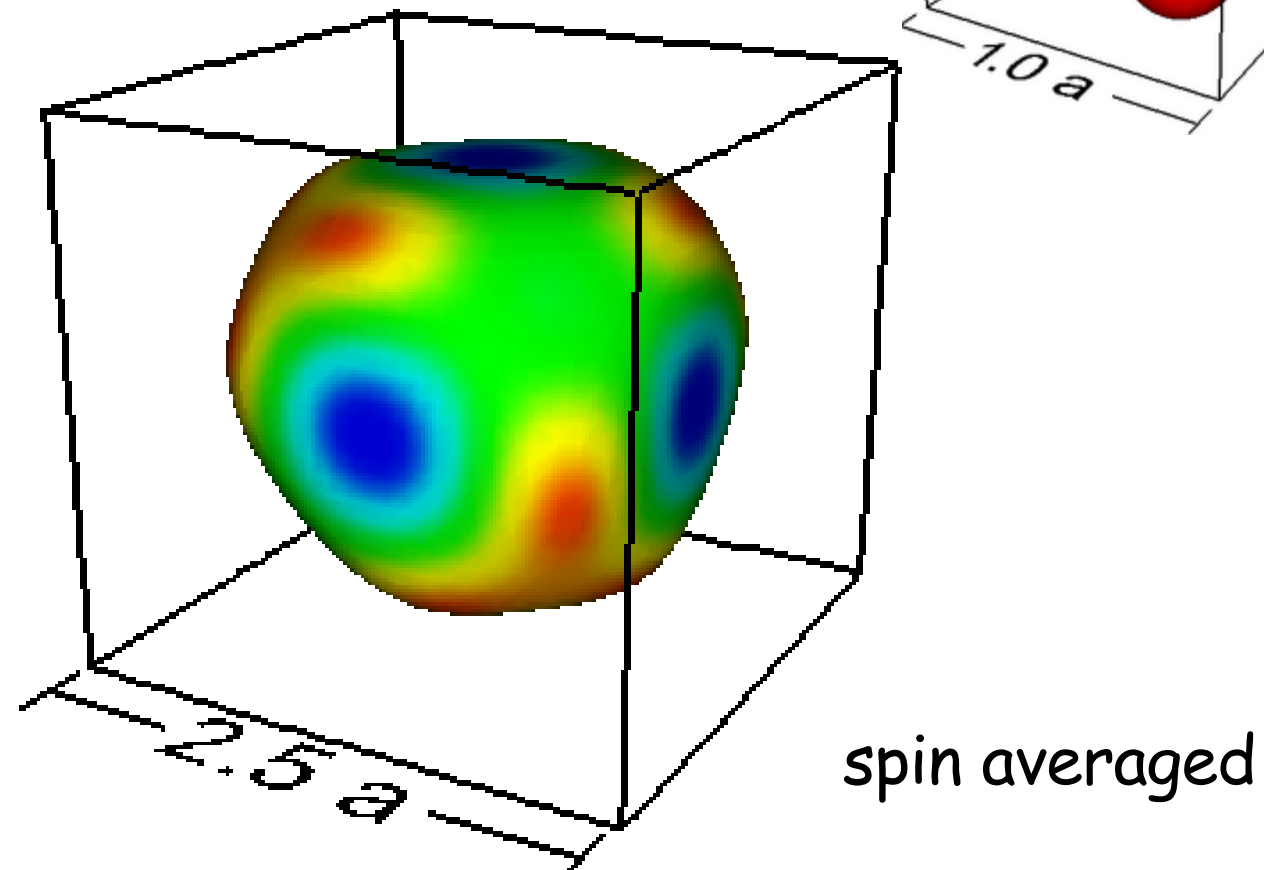
Mn + hole



• J. Schneider et al., PRL 59, 240 (1987)

Broken inversion symmetry

- Inversion asymmetry
 - bulk (Ga v.s. As)
 - impurity location
 - surface



How to control a spin

- magnetic field

$$H_B = g \mu_0 \mathbf{J} \cdot \mathbf{B}$$

- strain

$$H_S = b \left[\epsilon_{xx} \left(J_x^2 - J^2/3 \right) + c.p. \right]$$

$$+ d \left[\epsilon_{xy} \left(J_x J_y + J_y J_x \right) + c.p. \right]$$

- electric field

$$H_E = \gamma \left[E_x \left(J_x J_y + J_y J_x \right) + c.p. \right]$$

Energy scales

- coupling to E fields

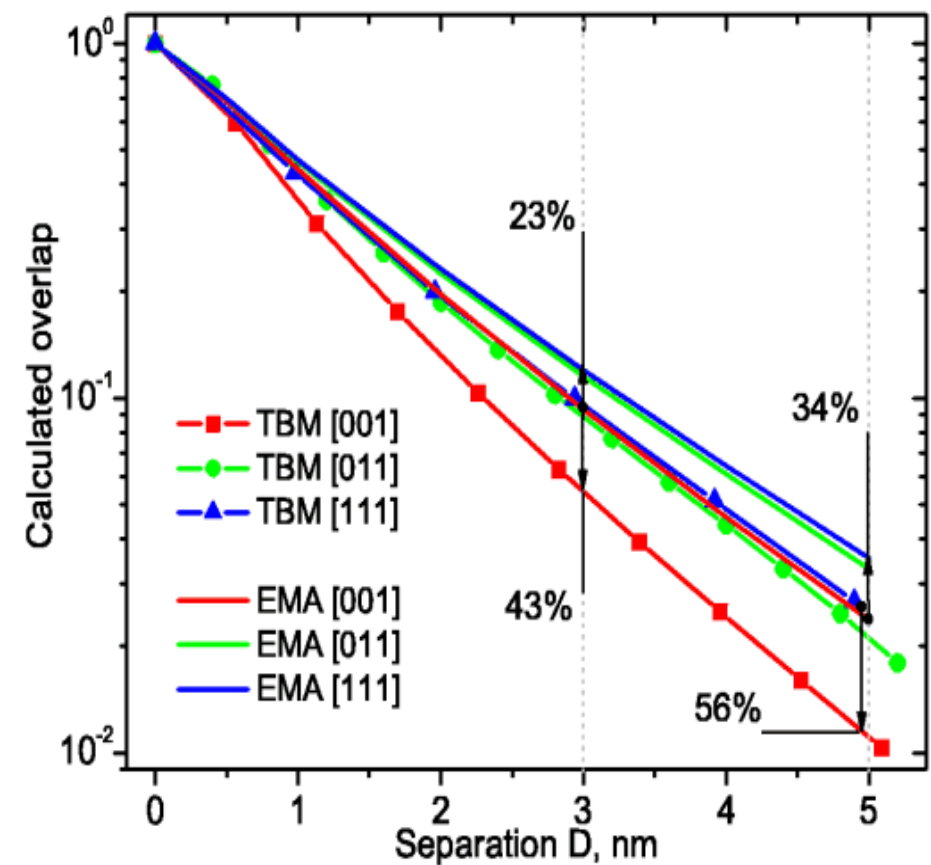
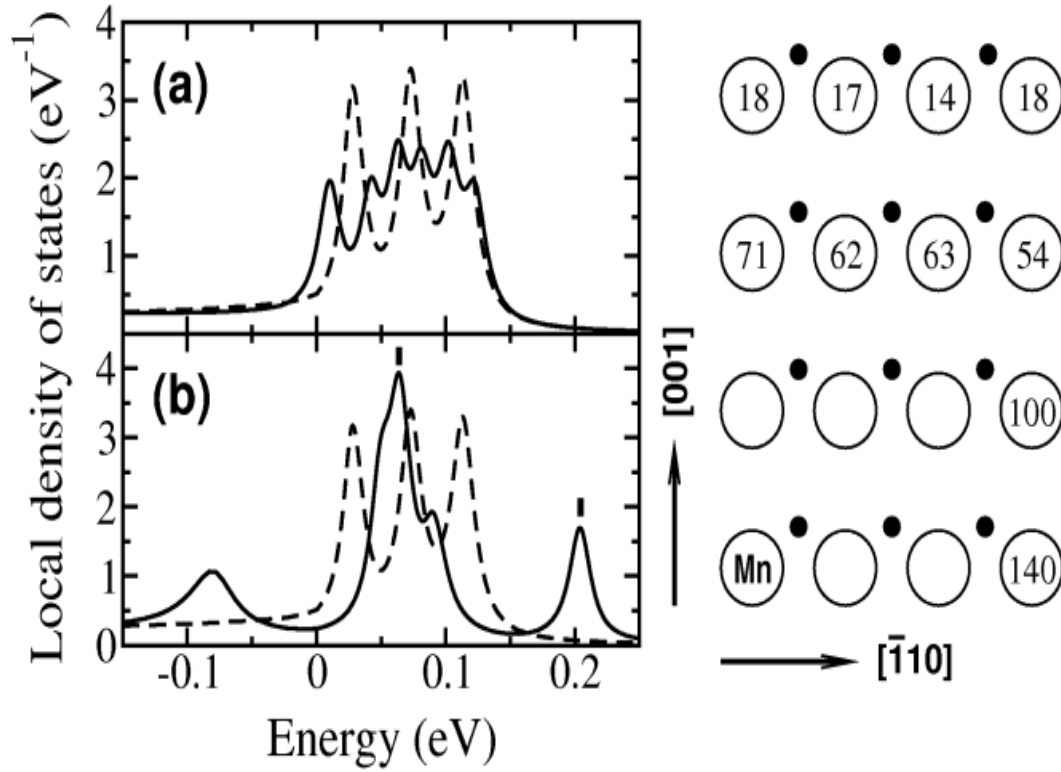
$$\langle \hat{n}, +1 | \mathbf{r} \cdot \mathbf{E} | \hat{n}, +1 \rangle \Rightarrow \gamma E = 160 \mu\text{eV}$$

$$E = 40 \text{ keV/cm} \Leftrightarrow B = 1 \text{ Tesla}$$

- Mn-Mn coupling

- ~10 - 100 μeV for 10 nm separation

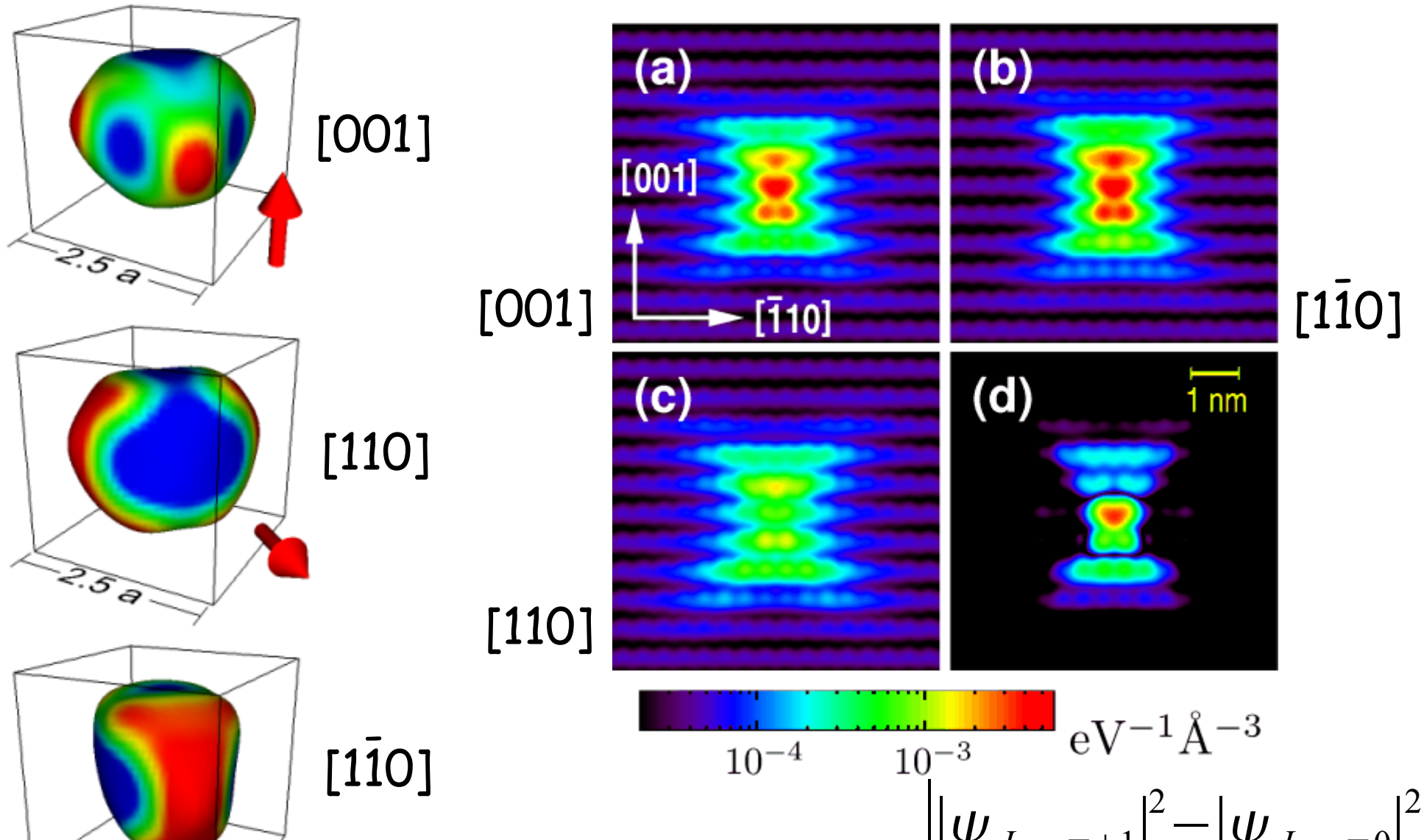
Mn-Mn overlap



J.-M. Tang and M. E. Flatté,
PRL 92, 047201 (2004)

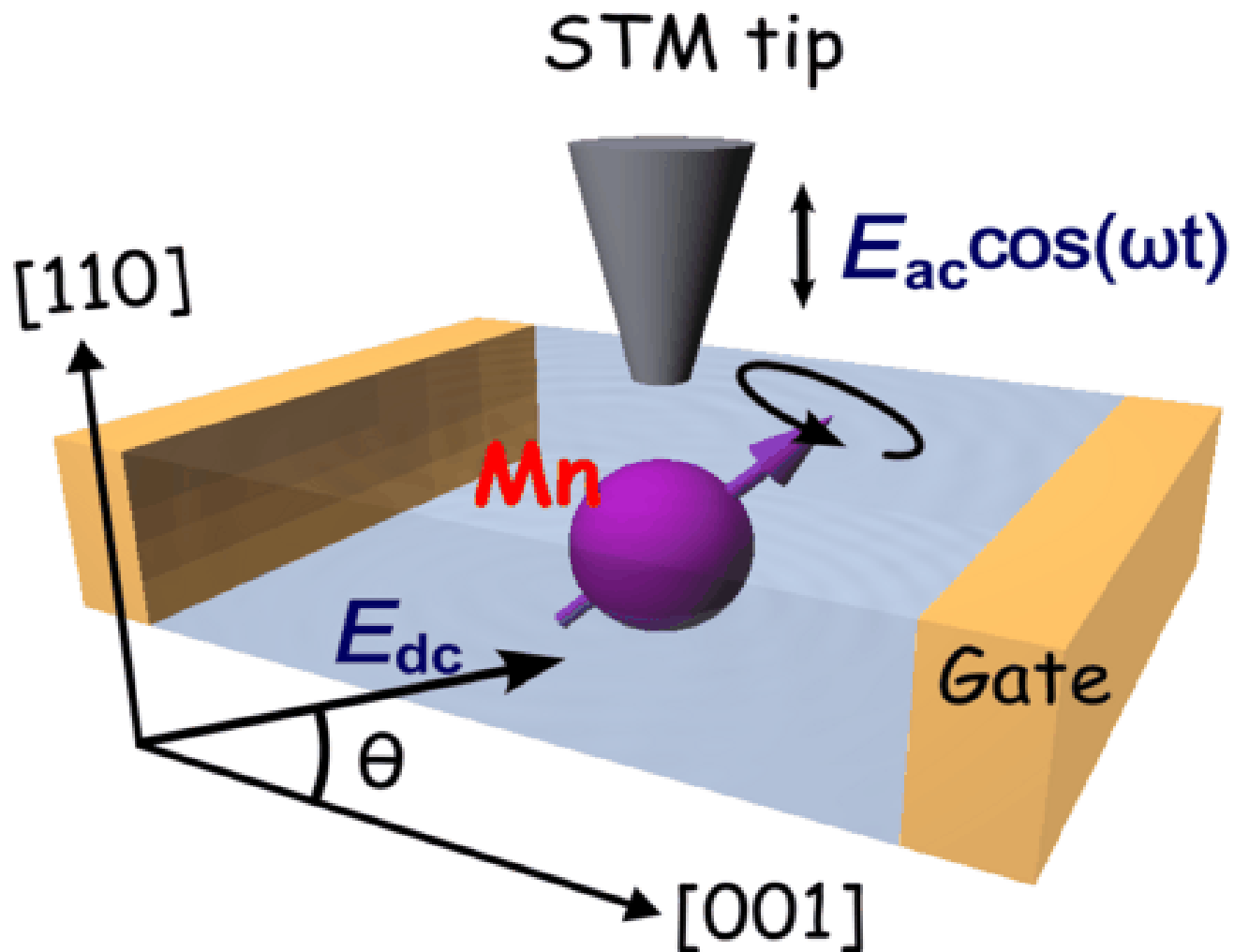
A.M. Yakunin, et al.,
PRL 95, 256402 (2005)

Spin-orientation-dependent LDOS



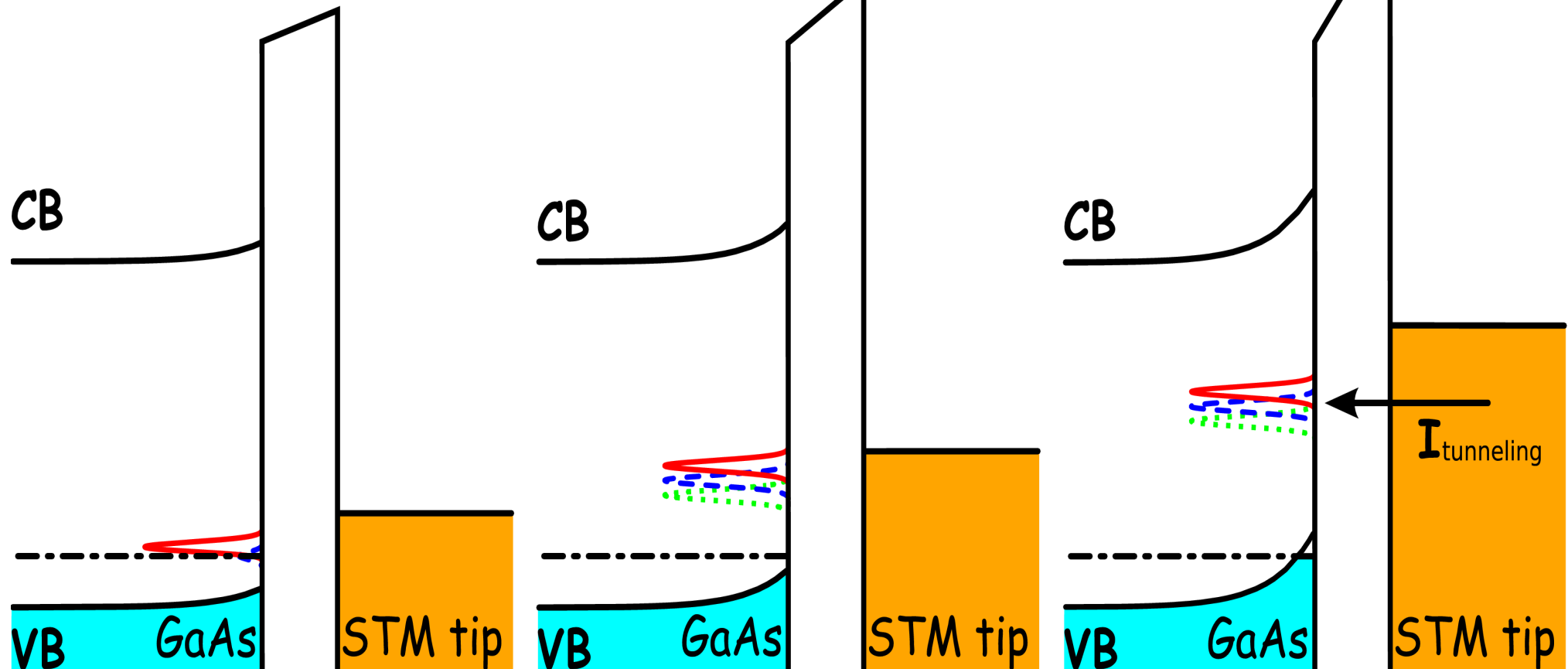
Showing the 4th layer away from the Mn layer
J.-M. Tang and M. E. Flatté, PRB 72, 161315 (2005)

Theorist's STM setup

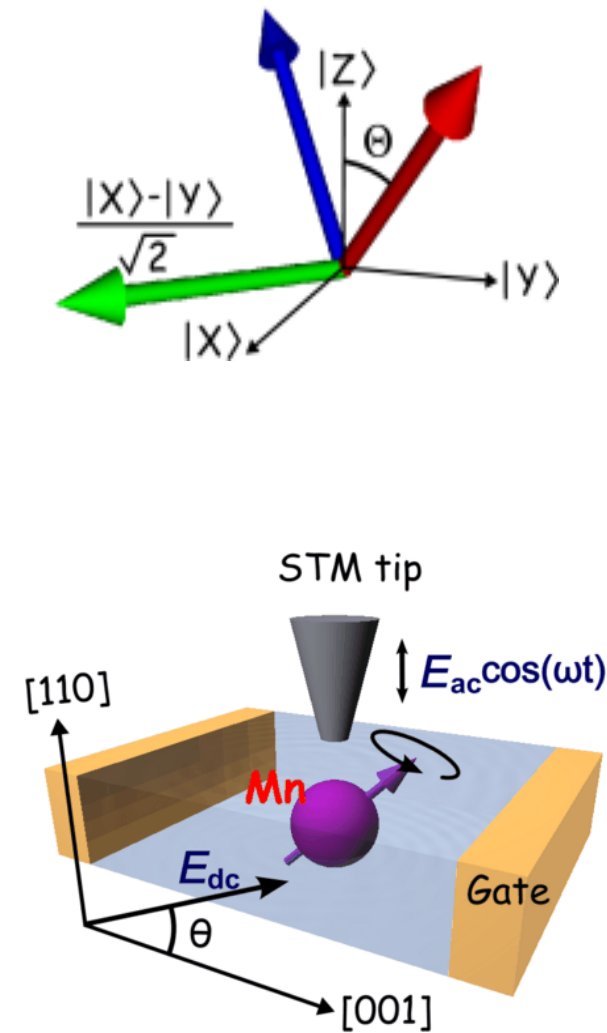
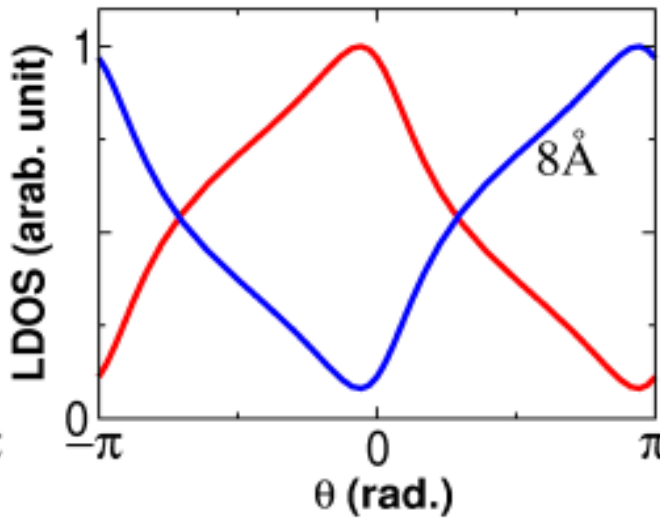
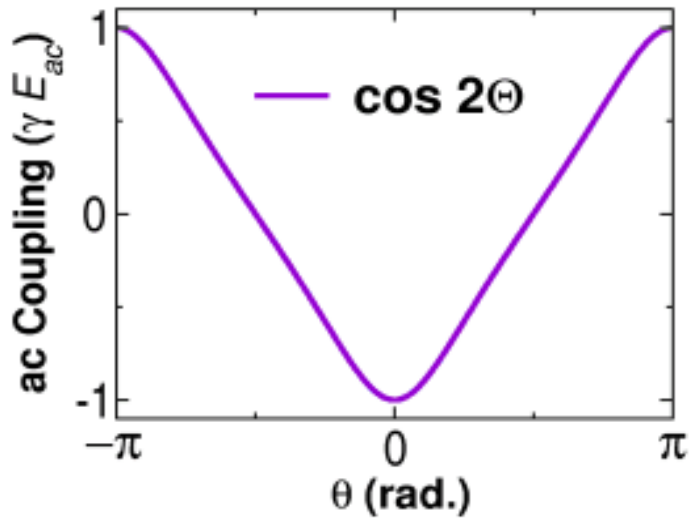
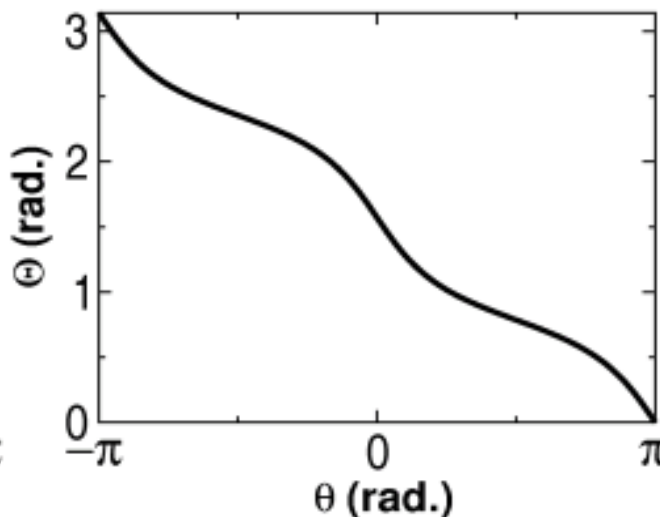
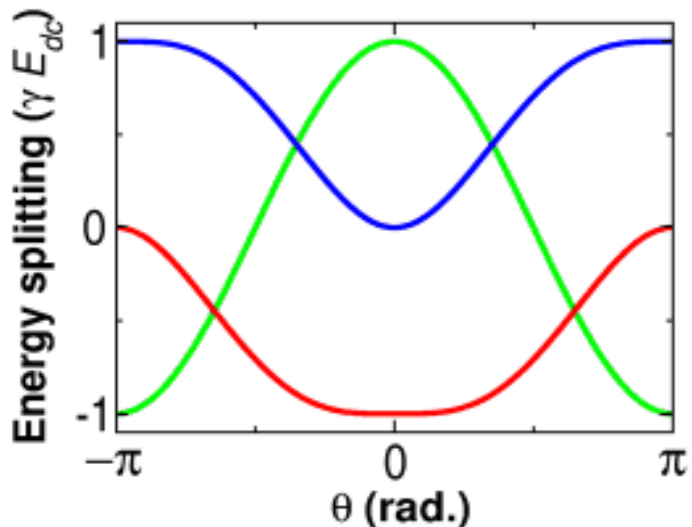


Manipulation scheme

(a) (b) (c)



Manipulation and detection



Summary

- The principal determinant of the anisotropic shape of the Mn wavefunction is the cubic symmetry of the lattice.
- The cubic symmetry is lowered by the dopant substitution, spin-orbit interaction, and bulk inversion asymmetry.
- The combination of spin-orbit anisotropy and broken inversion symmetry leads to the possibility of controlling the spin state of an ionic spin in a solid using electric or strain fields.